

ANNUAL TECHNICAL REPORT 1985
on
Earthquake Monitoring of Eastern and Southern Washington

September 1985

Geophysics Program
University of Washington
Seattle, Washington

This report was prepared as an account of work sponsored by the United States Government. Neither the United States nor the Department of Energy, nor any of their employees, nor any of their contractors, subcontractors, or their employees, makes any warranty, express or implied, or assumes any legal liability or responsibility for the accuracy, completeness or usefulness of any information, apparatus, product or process disclosed, or represents that its use would not infringe privately-owned rights.

By acceptance of this article, the publisher and/or recipient acknowledges the U.S. Government's right to retain a non-exclusive, royalty-free license in and to any copyright covering this paper.

PREPARED FOR THE U.S. DEPARTMENT OF ENERGY
UNDER CONTRACT NO. EY-76-S-06-2225
TASK AGREEMENT NO. 39

and

FINAL REPORT FOR:
THE U.S. NUCLEAR REGULATORY AGENCY
CONTRACT NO. NRC-04-81-177

QE
535,2
U6
A557
1985

TABLE OF CONTENTS

I.....Introduction and Operations3

II.....Seismicity9

III.....Structural Studies.....19

IV.....Vertical Seismic Profiling.....26

V.....Special Studies46

Appendix I.....Eastern Washington Catalog 1981-1982

Appendix II.....Station "up-time" Plots.....

Contributions by:

Peggy Browne

Dave Glover

Eric Lanning

Stephen Malone

Tony Qamar

Jim Zollweg



INTRODUCTION AND OPERATIONS

Introduction

This report covers the operations and research performed for D.O.E. and the N.R.C. by the University of Washington Geophysics Program on the seismicity and structure of eastern and southern Washington and northern Oregon for the year, July 1, 1984 to June 30, 1985. These contracts help support parts of the Washington state regional seismograph network. There are presently 111 stations in Washington and northern Oregon whose data are telemetered to the University for recording, analysis and interpretation. The Department of Energy supports the stations on the east flank of the Cascades and throughout eastern Washington. The Nuclear Regulatory Commission has supported stations in southern Washington and northern Oregon. Other major parts of the network are supported by the U.S. Geological Survey.

Section I of this report covers the operation of the network including station maintenance, data processing and telemetry problems in eastern Washington and the Washington-Oregon border area. The seismicity of the past year and a description of the catalog is covered in section II. The first part of section III is a brief description of our results from the joint USGS-Rockwell-UW refraction experiment carried out in August 1984 (An addendum to this report is the Master's Thesis by Dave Glover entitled *Crustal Structure of the Columbia Basin, Washington from Borehole and Refraction Data.*) The latter part of section III describes how these refraction experiment results are used to modify the velocity structure models used for locating earthquakes in Eastern Washington. Section IV is an abstract of our research in vertical seismic profiling. The Doctoral Dissertation of Eric Lanning entitled *Estimating Seismic Attenuation Using VSP Measurements* is included as an addendum to this report. Section V includes both a preliminary study of an unusual earthquake sequence near Vantage which has taken place during the past year, as well as a study of an earthquake sequence that took place near the Powder River landslide in northeastern Oregon. The appendices include the earthquake catalog for 1984-1985 and a

monthly listing of the station 'up-times' for the eastern Washington network.

Network Operations

Several significant changes have been made during the past year to our operation procedures. In December 1984 we decided to discontinue our maintenance contract with Stanwyck Corp. and hire our own staff technician to live and work in the Tri-Cities area. We hired a technician, Jim Hudspeth, who had worked with us previously and was familiar with our equipment. We provide him with a truck and test equipment. He has moved to Kennewick and from there can reach most of our stations in a minimum of two hours and all of them in four hours. We also hired another technician, Jack Libby, to work at the University in Seattle, primarily to help with the field work on the west side of the Cascades (USGS supported stations), but also for lab work on instrument repair, recording equipment repair, and general shop maintenance. This situation has worked out well providing fast service to "down" stations, as well as early diagnoses of problems.

At the first of the year the final Develocorder film recorder was taken off line. We continuously record several stations on Helicorders as backup to the digital on-line system. We also monitor the quality of each telemetry with frequent discriminator checks as well as the real-time P-picker statistics.

Table I-1 is a synopsis of the number of times the certain stations were visited during the course of the year. This information was taken from our log file which documents the maintenance, repair, or adjustment history of our seismic stations. It is simply a quick reference to particularly troublesome stations which required numerous visits. The site names with the R suffix are major receiving sites, some being seismic stations, and others being receiver sites only. There are several other listings which do not have the R extension and are receiver-repeater sites only. Some stations in eastern Washington required minimal service during the year and are not listed in this table. All stations supported by DOE are listed in Table I-2 and are shown in Figure I-1. Detailed plots of station history as determined from the diagnostics output of the real-time P-picker are given in Appendix II of this

report.

DYH	2	NEL	2	CBWR	6	MDW	2
HHH	3	OTH	2	SLH	1	PEN	2
MTM	5	WEN	1	VGB	6	WRD	1
PLN	3	AUG	3	WNS	2	GBL	3
JBO	2	ETP	1	FOX	2	MFW	1
NAC	4	NEW	1	ODS	3	OMK	2
PRO	2	SAW	1	PAT	5	SYR	1
WAT	4	WGW	2	WPW	2	YAK	8
ASR	2	AUGR	6	CRF	3	DY2	4
JUN	2	WIW	3	FPW	3	MOX	3
VTG	4	VCR	6				

Eastern Washington

The operation of the eastern Washington seismic network was fairly routine this year, providing good quality data with no extended outages of any stations. During July and August 1984 the USGS did a refraction study of the Hanford area and the University installed three temporary telemetry stations. After the refraction survey two of these stations (MOX & WNS) were retained as permanent stations. We installed solar battery chargers at MOX and WNS which worked well throughout the winter. A total of eight more stations were converted to solar power during the year. We are currently evaluating whether or not the solar panels will save time and expense compared to the use of non-rechargeable aircells.

There were two network changes in north Central Washington. FPW and OMK were moved to new locations. FPW became NEL and is now radioed to CBW. OMK became FOX and is radioed to DY2 (which was moved a short distance from DYH) and these are then radioed to CBW. This eliminated two more phone drops and prepares CBW to link with the BPA telemetry system.

In the south-central Washington area there were two other changes. RPK (an old Oregon PGE station) was reinstalled at its original location and is radioed to VGB. GL2 replaced GLD and is now radioed to AUG. GL2 now fills a large gap in the array in the south-central area, and the station is calibrated, using an S-13 seismometer. Seismometers

TABLE I-2 DOE Supported or Related Stations

	LAT	LONG	EL	NAME
AUG	45 44 10.0	121 40 50.0	0.865	Augsburger Mountain
BRV	46 29 07.2	119 59 29.4	0.200	Black Rock Valley
CBW	47 48 25.5	120 01 57.6	1.160	Chelan Butte
CRF	46 49 30.6	119 23 18.0	0.260	Corfu
DYH	47 57 37.8	119 46 09.6	-	Dyer Hill
ELL	46 54 35.0	120 34 06.0	0.805	Ellensburg
EPH	47 21 07.8	119 35 46.2	0.628	Ephrata
EST	47 14 16.8	121 12 21.8	0.756	Easton
ETP	46 27 53.4	119 03 32.4	0.250	Eltopia
ETT	47 39 18.0	120 17 36.0	0.439	Entiat
FPW	47 58 09.0	120 12 46.5	0.352	Fields Point
GBL	46 35 51.6	119 27 35.4	0.330	Gable Mountain
GL2	45 57 50.0	120 49 15.0	1.000	New Goldendale
HHW	46 10 59.0	119 22 59.0	0.415	Horse Heaven Hills
MDW	46 36 48.0	119 45 39.0	0.330	Midway
MFW	45 54 10.8	118 24 21.0	-	Milton-Freewater
MOX	46 34 38.0	120 17 35.0	0.540	Moxie City
NAC	46 44 03.8	120 49 33.2	0.738	Naches
NEW	48 15 50.0	117 07 13.0	1.000	USGS - Newport
ODS	47 18 24.0	118 44 42.0	-	Odessa
OMK	48 28 49.2	119 33 39.0	0.421	Omak
OTH	46 44 20.4	119 12 59.4	0.260	Othello
PAT	45 52 50.1	119 45 40.1	0.300	Paterson
PEN	45 36 43.2	118 45 46.5	-	Pendleton
PLN	47 47 04.8	120 37 58.8	2.000	Plains
PRO	46 12 45.6	119 41 09.0	0.552	Prosser
RPK	45 45 42.0	120 13 50.0	0.330	Roosevelt Peak
RSW	46 23 28.2	119 35 19.2	1.037	Rattlesnake Mountain
SAW	47 42 06.0	119 24 03.6	-	St. Andrews
SYR	46 51 46.8	119 37 04.2	-	Smyrna
TBM	47 10 10.0	120 35 58.0	-	Table Mountain
VGB	45 30 56.4	120 46 39.0	0.729	USGS - Gordon Butte
VGT	45 08 59.4	122 15 55.2	0.993	USGS - Goat Mtn.
VIP	44 30 29.4	120 37 07.8	1.731	USGS - Ingram Point
VTG	46 57 28.8	119 59 14.4	0.208	Vantage
VTH	45 10 52.2	120 33 40.8	0.773	USGS - The Trough
WA2	46 45 24.2	119 33 45.5	0.230	Wahluke Slope
WAT	47 41 55.0	119 57 15.0	0.900	Waterville
WBW	48 01 04.2	119 08 13.8	-	Wilson Butte
WEN	47 31 46.2	120 11 39.0	1.061	Wenatchee
WGW	46 02 40.8	118 55 57.6	-	Wallula Gap
WIW	46 25 48.8	119 17 13.4	0.130	Wooded Island
WNS	46 42 37.0	120 34 30.0	1.000	Wenas
WPW	46 41 53.4	121 32 48.0	1.250	White Pass
WRD	46 58 11.4	119 08 36.0	-	Warden
YAK	46 31 15.8	120 31 45.2	0.619	Yakima

SEISMICITY 1984 - 1985

Introduction

During the past year the level of seismicity in Washington state and northern Oregon has been typical of the last five years. No damaging earthquakes occurred in Washington state or northern Oregon. The largest magnitude earthquake was a magnitude 3.9 earthquake which occurred in the Washington-Oregon border area near Hermiston, Oregon on February 10, 1985.

In the period July 1, 1984 to June 30, 1985 we processed 2173 seismic events. 1652 of these were located within the area of eastern Washington and southern Washington/northern Oregon shown in Figure I-1. 1020 of the events were earthquakes that occurred during two eruptions of Mount St. Helens on Sept. 9-12, 1984 and May 27-June 5, 1985. These and 40 earthquakes that occurred at Elk Lake, 30 km NNW of Mount St. Helens, are not discussed in this report. Here we include 277 blasts and 326 earthquakes in the two areas shown in Figure I-1. The 326 earthquakes exclude Mount St. Helens events less than magnitude 3.0 and Elk Lake events less than magnitude 1.5.

General Seismicity

Figures II-1 and II-2 show blasts and suspected blasts within the area covered by this report. Blasts are identified by their characteristic source locations and recorded waveforms as well as receiving confirmation from blasting contractors. The 326 earthquakes for the period are shown in Figures II-3 and II-4 and are listed in a catalog as Appendix 1 of this report. Although Figures II-1 and II-2 show all blasts, only blasts with $M > 2.5$ are listed in the catalog.

All earthquakes for the period had magnitudes less than 3.5 except one ($M = 3.9$) which occurred February 10, 1985 in northern Oregon, 75 km southwest of Pasco, Washington. It was felt in Oregon on the Boardman Bombing Range. This event has a focal depth of 18km, an unusual depth for earthquakes in eastern Washington. While the station

distribution is not ideal for locating this event (azimuthal gap of 210°), because of its size it was well enough recorded to give us some confidence in this location. A focal mechanism for this event is shown in Figure II-5 and while not well constrained, shows almost pure strike slip faulting on vertical nodal planes northwest-southeast and northeast-southwest. No aftershocks were located near this epicenter which is similar to other larger events in southern Washington in previous years.

As in former years the most active region in eastern Washington was near Entiat, just south of Lake Chelan. A group of 68 earthquakes were located there and occurred uniformly in time during the year. Another persistent source of earthquakes, noted also last year, occurred 35 km southwest of Grand Coulee. Scattered earthquakes also occurred northwest of Yakima, an area which had two magnitude 3.8 earthquakes last year.

Numerous earthquakes occurred to the south of Vantage, Washington in the Saddle Mountains region. This is a known active area and is traversed by the the Saddle Mountains thrust fault. The epicenters that occurred in the region this year lay somewhat west of last year's epicenters.

On October 31, 1984 a swarm of earthquakes began in a new region a few kilometers north of Vantage. We have located 26 of these events in a tight cluster as of June 30, 1985. Two of these reached magnitude 3.3. The earthquakes north of Vantage have provoked a special study and are discussed in more detail in section V.

Most of the activity we have located this year in southern Washington and northern Oregon lies along the north-northwest trending Mount St. Helens seismic zone (Fig. II-4). In addition, a number of earthquakes were located along the Columbia river north of Portland, Oregon.

Catalog

Appendix I is a catalog of located events between July 1, 1984 and June 30, 1985 in the two regions of eastern Washington and southern Washington/northern Oregon shown

in Figure I-1. Mount St. Helens earthquakes (46.15 - 46.25N, 122.10 - 122.27W) with magnitudes less than 3 are not included nor are Elk Lake earthquakes (46.325 - 46.375N, 122.22 - 122.27W) less than magnitude 1.5. In addition, only blasts with magnitude equal to or exceeding 2.5 are listed. The locations reported in the catalog have been determined using a hypocenter computer program *spong*, which is an adaptation of a program originally written by Bob Herrmann at Saint Louis University. There is a special depth adjustment algorithm for events with poorly controlled shallow depths such as those sometimes found in the central Pasco Basin. Different seismic velocity models are used to locate earthquakes in different regions. Table II-1 lists the fundamental parameters used for the new velocity models in each region. Individual minor station corrections were determined for each model but these are not listed in the table. See section III of this report for a detailed discussion of the E3 and N3 models. The columns in the catalog are generally self-explanatory except that the following features should be noted:

- a) The origin time listed is that calculated for the earthquake on the basis of multistation arrival times. It is given in Coordinated Universal Time (UTC), identical to Greenwich Civil Time; in hours:minutes (TIME); and seconds (SEC). To convert to Pacific Standard Time (PST) subtract eight hours, or to Pacific Daylight Time subtract seven hours.
- b) The epicenter location is given in north latitude (LAT) and west longitude (LONG) in degrees and minutes.
- c) In most cases the DEPTH, which is given in kilometers, is freely calculated by computer from the arrival-time data. In some instances, the depth must be fixed arbitrarily to obtain a convergent solution. Such depths are noted by an asterisk (*) in the column immediately following the depth. A \$ or a # following the depth mean that the maximum number of iterations has been exceeded without meeting convergence tests and the depth has been fixed.

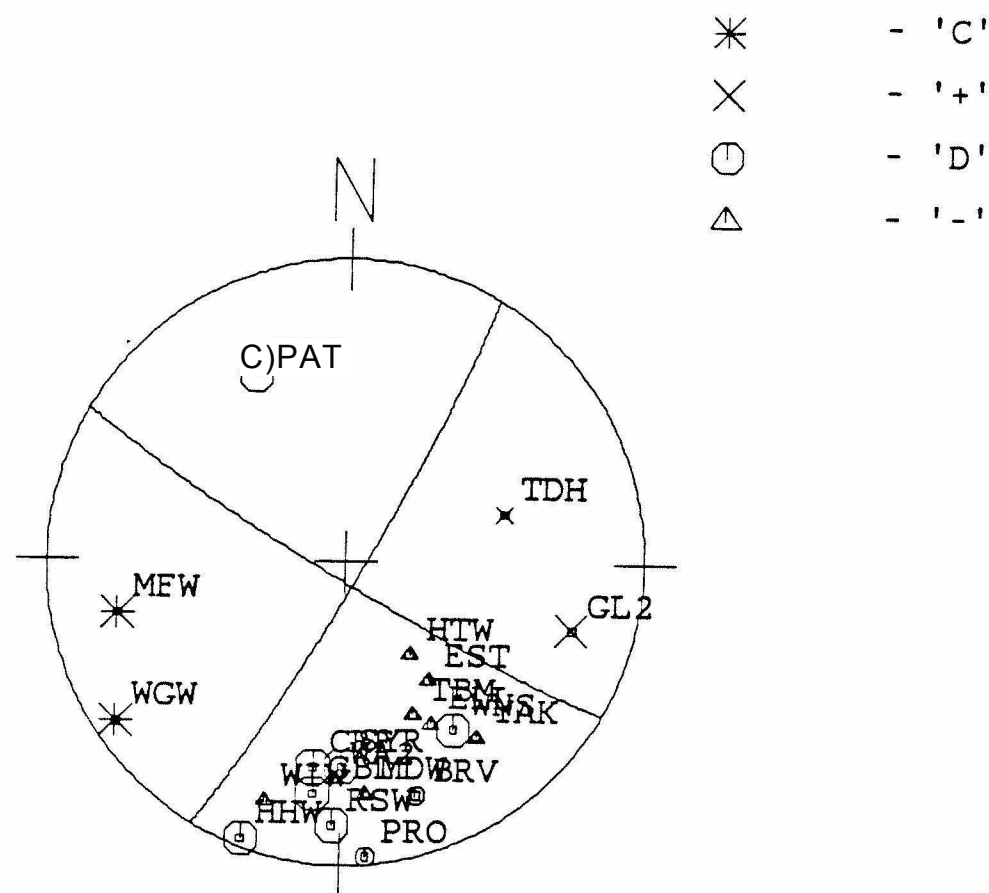


Figure II-5. First motion patterns and potential fault-plane solution for the magnitude 3.8 earthquake of Feb. 10, 1985 near Hermiston, Oregon. The plot is an upper-hemisphere equal area stereo projection.

STRUCTURAL STUDIES

Studies of the velocity structure of eastern Washington have been completed using the refraction data from the cooperative USGS refraction line run in the summer of 1984. The following is the abstract from David Glover's Master's Thesis. The entire thesis is included as an addendum to this report.

Crustal Structure of the Columbia Basin, Washington

from Borehole and Refraction Data

Abstract by: David Glover

A three-dimensional five-layered crustal model of the Columbia Basin has been constructed based on refraction data collected in August, 1984 by the USGS, Rockwell Hanford Operations, and the University of Washington. The USGS deployed a 260km-long line running NE-SW through the central basin with dense station spacing. The University of Washington set up unreversed refraction lines with sparse station spacing concentrated to the west of the USGS line while Rockwell Hanford Operations deployed stations to the east. Starting with the dense data from the reversed USGS line, intercept times and crossover distances were used to create a two-layered model. This model was then expanded to five layers, including a low-velocity layer beneath the basalts, by using an iterative scheme of two-dimensional forward ray-tracing and data from several deep boreholes.

The model consists of a 0.5km-thick, 3.7km/s surface layer overlaying the basalts, which have an average velocity of 5.18km/s. The average velocity for the low-velocity layer ranges from 4.6km/s to 5.0km/s. Deep borehole sonic logs confirm the existence of this low-velocity layer and are used to fix the depth to the bottom of the basalts in the northern region. Analysis of the refraction data reveals that the basalts extend to a depth of approximately 5.4km in the central basin and thin to a depth of 1.8km in the northeast and 0.8km in the northwest. The top of the 6.2km/s crystalline basement refractor extends to depths between 10km and 11km in the central basin and shallows to the north. Shallowing of the basement rock was confirmed by additional refraction data collected from a local mine in

the northern part of the study area. A deep-crustal layer with an average velocity of 7.2km/s begins at depths of about 18km in the south increasing to approximately 22km in the northern part of the study area.

Velocity Models for Earthquake Locations

The above research has prompted a reevaluation of the velocity models we have been using for earthquake locations in eastern Washington. Since 1977 we have been using a set of three slightly different velocity models for locating earthquakes east of Puget Sound. These models were based on small scale studies of the region using both earthquakes and quarry blasts as recorded on our network stations. The study mentioned above using dense arrays for data collection have provided enough detailed information that our regional velocity models can be adjusted to take into account the new data. New models have been developed for the *N* and *E* areas but not for the *C* area. See Figure I-1 for the boundaries of the areas covered by the three different velocity models.

The procedure for modifying the eastern Washington velocity models consists of determining an average flat layer model with constant velocity in each layer which would best approximate the complex three dimensional model developed in the above work. We then used a series of blasts with known locations and a distribution of well recorded earthquakes to develop station corrections for each of these models. Since the travel-time calculation program which we use for routine locations can not be used with models with low velocity zones, we have neglected including this zone in our models. Instead, we extend the basalt layer down to the depth of the crystalline basement layer and account for the existence of the low velocity zone by station corrections.

Model N3

While the detailed refraction study mentioned above was concentrated in the southern part of the Plateau, lines extending north of the Saddle Mountains provided enough data to modify the model we have been using. In particular, an additional deep crustal layer with a velocity of 6.4 km/sec was added as well as placing the Moho deeper than previously

thought. Table III-1 lists the velocity model we have been using for the past several years, N1, as well as the new revised one, N3.

TABLE III-1 Northeast Velocity Structures

Old Model (N1)		New Model (N3)	
V (km/sec)	Depth (km)	V (km/sec)	Depth (km)
5.10	0.0	5.1	0.0
6.05	0.5	6.1	0.5
7.2	19.0	6.4	14.0
8.0	24.5	7.1	24.0
		7.9	38.0

Using the new N3 structure, residuals from 7 blasts and 16 earthquakes (see Table III-2) were calculated to be used as station corrections. This calculation was done in an iterative fashion. Using the blasts with known locations, their origin times were determined using only arrival times from stations within 30km. Since the upper part of the new model is the most reliably determined and very close to the old model, these origin times should be fairly accurate. Residuals were then calculated for all stations by subtracting observed arrival times from predicted ones using the new model. Using these residuals as station corrections, origin times for these blasts were recalculated and a suite of well recorded earthquakes were located, this time using only stations within 50km. Station residuals were then again determined for all stations and added to those from the previous iteration. This cycle was repeated yet another time, but using all arrivals from stations within 100km of the sources. A final iteration used all arrivals. The blasts and earthquakes used for this procedure are listed in Table III-2.

This iterative procedure starts by using data from parts of the structure we have the most confidence in and progressively adds more data from areas less well determined. An advantage of the technique is that it allows one to estimate the reliability of the results at each step along the way. By plotting residuals versus distance for all blasts and shallow earthquakes, one can qualitatively judge the accuracy of various parts of the velocity model. This technique confirmed the existence of the deeper layers of the N3 model.

Table III-2 Events for N3 Station Corrections

DAY	TIME	SEC	LAT	LON	DEPTH	MAG	NS/NP	RMS	Q	MODEL	TYPE
81/05/01	17:16	53.51	47 36.80	119 53.69	0.05#	0.	21/22	0.20	BC	N3	X
81/06/29	0:19	25.02	47 1.10	120 13.22	0.05#	2.7	30/30	0.36	CC	N3	X
82/02/02	0:29	55.05	47 52.63	118 7.85	0.05#	1.5	12/13	0.35	CC	N3	X
83/02/02	20:57	64.87	46 54.84	119 7.38	0.05#	1.7	21/22	0.36	CB	N3	X
83/06/17	23:09	19.67	48 5.60	118 58.22	0.05#	2.8	17/19	0.26	BC	N3	X
83/11/23	0:06	1.89	48 17.63	119 25.50	0.05#	1.3	8/09	0.13	AC	N3	X
83/11/29	21:45	57.79	48 17.63	119 25.50	0.05#	1.5	8/09	0.15	BC	N3	X
80/06/18	11:41	29.03	48 36.90	119 36.99	6.48	3.0	6/06	0.09	CD	N3	F
80/12/03	23:46	22.94	47 41.09	120 8.31	0.65	2.2	25/30	0.16	BC	N3	
81/03/07	19:27	62.74	47 49.10	119 49.10	3.29	2.5	18/23	0.11	AC	N3	
81/05/15	22:44	8.36	47 14.83	118 51.12	0.02*	2.0	19/21	0.29	BC	N3	
81/05/26	21:10	23.91	47 39.51	120 17.24	0.77	2.6	24/24	0.18	BC	N3	
81/07/22	6:05	50.39	47 46.74	120 17.37	8.90	3.0	28/28	0.29	BB	N3	F
81/07/30	15:38	67.04	47 39.68	120 10.57	0.51	2.3	26/27	0.29	BB	N3	
81/10/25	3:20	63.68	47 45.55	120 11.95	7.16	3.2	24/24	0.18	BB	N3	F
81/12/21	2:46	61.15	47 49.46	119 37.09	2.54	2.2	23/26	0.24	BC	N3	
82/01/04	8:43	52.09	47 13.93	120 38.60	5.09	2.7	37/39	0.22	BC	N3	
82/10/14	8:53	39.97	47 42.89	120 11.57	3.77	2.4	22/25	0.14	AC	N3	
82/10/16	1:31	15.78	47 31.21	120 38.64	6.30	2.1	29/32	0.19	BC	N3	
83/06/10	18:19	67.97	47 39.66	120 17.05	4.52	2.7	22/24	0.28	BA	N3	
83/07/09	9:49	18.15	47 41.93	120 11.16	0.64	2.2	24/27	0.29	BB	N3	
83/07/24	14:20	51.69	47 42.23	120 6.21	3.49*	2.5	23/24	0.28	BC	N3	
83/10/28	7:57	51.90	47 31.48	120 39.14	6.81	2.2	26/29	0.30	BC	N3	

Model E3

A similar procedure for modifying the E1 model to a new one was followed for the central part of the basalt plateau using 14 blasts and 14 earthquakes. In this case the results of the cooperative refraction experiment can be applied much more directly to the definition of a flat layered velocity model. The basalt and underlying low-velocity sedimentary layers change thickness quite dramatically throughout this part of the state. Since we must use uniform flat-lying layers for our travel-time calculation routine, an approximation of these layers is necessary. Table III-3 shows the model used since 1977, E1 as well as the new model derived from our recent work, E3.

TABLE III-3 Southeast Velocity Structures

Old Model (E1)		New Model (E3)	
V (km/sec)	Depth (km)	V (km/sec)	Depth (km)
3.70	0.0	3.70	0.0
4.70	0.8	5.15	0.4
5.15	1.2	6.10	8.5
6.05	7.5	6.40	13.0
7.20	19.0	7.10	23.0
8.00	28.0	7.90	38.0

Again, the deeper layers for the new model are significantly different than those in the old model. Also, the basalt layer (velocity of 5.15 km/sec) is thicker, extending from 0.4 km down to 8.5 km depth. The lack of a low velocity zone in this model is only because our location routine does not presently have the capability to calculate travel-times through such a zone. During the next year, we plan to develop this capability as well as test the necessity of its inclusion.

Similar to the N3 model, station corrections for the E3 model were developed in an iterative fashion using blasts at known locations to begin with and then both blasts and well recorded earthquakes at the end. Table III-4 gives information about these events. Table III-5 is a list of station corrections for most of the stations in the eastern Washington network for both the N3 and E3 models.

Table III-4 Events for E3 Station Corrections

DAY	TIME	SEC	LAT	LON	DEPTH	MAG	NS/NP	RMS	Q	MODEL	TYPE
81/06/29	0:19	23.82	47 1.10	120 13.22	0.05#	2.7	33/33	0.31	CC	E3	X
80/07/24	17:14	16.24	46 17.20	119 32.60	0.05#	2.3	13/13	0.20	BC	E3	X
81/12/08	1:43	43.13	46 14.78	118 54.51	0.05#	1.5	20/22	0.69	DC	E3	X
82/02/20	0:59	16.42	46 45.98	118 0.40	0.10#	2.1	21/21	0.41	CD	E3	X
82/10/12	1:30	21.31	45 59.30	119 18.50	0.05#	0.	24/24	0.20	BC	E3	X
82/11/02	22:04	24.86	46 27.65	119 1.71	0.05#	1.3	21/22	0.38	CC	E3	X
83/02/02	20:57	63.87	46 54.84	119 7.38	0.05#	1.7	26/27	0.24	BB	E3	X
83/06/07	22:56	29.04	46 4.70	119 36.04	0.10#	1.8	14/14	0.28	BC	E3	X
83/10/24	23:01	61.12	46 14.24	119 20.98	0.05#	1.7	11/12	0.42	CB	E3	X
83/10/25	23:11	41.66	46 49.76	120 19.55	0.05#	2.4	24/24	0.33	CC	E3	X
84/08/19	10:59	59.84	46 58.23	119 11.74	0.02#	2.7	31/31	0.23	BA	E3	X
84/08/19	11:31	60.03	46 40.56	119 27.96	0.04#	2.4	31/31	0.15	AA	E3	X
84/08/23	9:03	60.09	46 20.87	119 50.29	0.02#	2.1	27/27	0.31	CC	E3	X
84/08/23	9:05	60.08	45 56.45	120 14.77	0.02#	2.3	30/30	0.29	BC	E3	X
80/11/19	21:35	23.97	46 56.96	119 28.18	0.02*	3.3	25/28	0.12	AC	E3	
80/12/03	6:58	46.90	46 55.17	119 21.93	1.96	2.6	25/28	0.24	BC	E3	
80/12/12	18:41	37.70	46 56.02	119 54.13	2.45	1.9	29/29	0.20	BB	E3	
81/02/19	17:19	23.13	46 40.78	119 18.36	0.03*	2.7	16/17	0.12	AC	E3	
81/02/27	22:45	32.62	46 56.68	119 33.53	0.50	2.7	23/23	0.19	BC	E3	
81/06/27	11:53	46.78	46 55.15	119 21.73	0.02*	2.3	20/21	0.16	BC	E3	
81/09/23	16:28	39.09	46 31.41	119 43.52	19.41	2.3	24/29	0.22	BA	E3	
81/09/28	0:54	22.42	46 57.67	119 39.80	1.02	2.6	23/25	0.17	BC	E3	
81/10/15	8:49	18.16	46 58.06	120 26.18	8.59*	2.3	28/29	0.17	BB	E3	
82/07/04	10:57	12.92	46 44.59	119 51.40	13.83	2.1	29/30	0.17	BB	E3	
82/09/10	0:44	26.02	46 49.14	119 25.21	2.90	2.6	28/28	0.15	AA	E3	
82/11/08	0:23	61.11	46 52.64	119 28.40	13.56	2.3	31/39	0.22	BA	E3	
83/05/16	11:47	45.54	46 49.39	119 21.93	1.99	2.6	28/29	0.25	BA	E3	
83/10/20	9:44	58.46	46 43.04	119 35.03	1.73	3.4	27/31	0.16	BA	E3	

Table III-5 Station corrections

Name	N3	E3	Name	N3	E3
CBW	0.00	-0.17	OMK	-0.03	0.55
CRF	0.22	-0.02	OTH	0.11	0.03
DAV	-0.44	-0.55	PAT	0.00	0.24
DYH	-0.03	-0.12	PEN	0.00	-0.08
ELL	0.59	0.39	PLN	-0.03	-0.12
EPH	-0.02	-0.26	PRO	0.75	0.14
EST	0.20	-0.10	RPK	0.00	0.10
ETP	-0.50	-0.20	RSW	0.22	0.09
ETT	-0.04	-0.44	SAW	-0.05	-0.57
FMW	-0.05	0.03	SYR	0.20	0.03
FPW	-0.09	-0.30	TBM	0.40	0.20
GBL	0.27	0.03	VTG	0.11	0.03
GL2	0.34	0.25	WA2	0.40	0.01
BDG	0.21	0.13	WAT	0.02	-0.28
GSM	0.82	0.26	WBW	0.00	-0.60
HTW	-0.27	-0.30	WEN	-0.03	-0.45
JCW	-0.10	-0.02	WIW	0.40	0.00
MDW	0.78	0.02	WPW	-0.04	-0.02
MFW	0.00	0.05	WRD	0.07	-0.02
NAC	0.55	0.44	YAK	0.47	0.48
NEW	-0.68	1.25	ODS	-0.23	-0.48

ESTIMATING SEISMIC ATTENUATION USING VSP MEASUREMENTS

During the past several years we have been involved in the study of in-situ seismic attenuation. A procedure for inverting Vertical Seismic Profiling (VSP) data for the vertical attenuation structure has been developed by Eric Lanning as his PhD degree research project. The acquisition of high quality VSP data was necessary for the testing of this procedure. Data from the Hanford area were not of high enough quality for use in developing the inversion technique. High quality data from a VSP survey in north Texas was acquired from the ARCO Research and Development Corporation as an experimental data set. After the technique was developed it was then applied to data from the Hanford area.

The following is the abstract from the PhD dissertation by Eric Lanning. Following the abstract is the final chapter from this dissertation on attenuation studies of data from a borehole on the Hanford reservation. The rest of the dissertation is included as an addendum to this report.

Abstract

by Eric Lanning

In this dissertation I present an inverse technique for estimating the in-situ seismic velocity and attenuation of subsurface formations using vertical seismic profiling measurements. The method is applied to a data set taken in a well in Northern Texas that penetrates a series of marine sedimentary formations.

Travel time determinations are made using what is known as a Front-Back Ratio (Crosson, 1984) where picking errors are shown to be less than ± 1 sample interval. The travel times along with the source and receiver locations are used in an iterative inversion scheme to compute the velocity structure using layered models, the model boundaries coinciding with the changes in lithology.

Least squares match filtering and predictive deconvolution are used to estimate information about the initial arrival at the seismometers on each shot assuming it to be a pure

p-wave. This information is used to correct for the variations in the source wave field during the survey and to reduce the effect of interference between multiple arrivals within the analysis time window. Amplitude spectra at each of the borehole depths are used to compute spectral ratio slopes which, along with the results of the velocity analysis, are used in a linear inversion for the subsurface attenuation.

The results of the inversion are compared with attenuation estimates made from travel time differences computed from the vertical VSP times and those found by integrating sonic log measurements. These two methods sample the subsurface at frequencies that differ by $>10^4$ Hz and the time difference is assumed to be due to velocity dispersion. It was found that the inverse technique provided good resolution of the attenuation at the length scale of the geologic formations and had error estimates that were an order of magnitude less than those for the drift time calculation.

Finally, the results of applying the analysis to data taken in a series of flood basalts of the Columbia River Plateau are shown. A number of serious acquisition problems were identified and only a crude estimate of the attenuation was possible.

Hanford VSP

(Chap 7 of Eric Lanning Dissertation)

Introduction

Located in southeastern Washington, the Hanford Nuclear Reservation has been the site of extensive drilling and coring operations. The reservation is on the Columbia River Plateau, a sequence of tholeiitic basalt lava flows. The Columbia River Basalt Group, the designation for the sequence of flows, was erupted between 6 and 16.5 million years ago and are believed to be the world's youngest flood basalts (Watkins, Baksi, 1974; Mckee, et al., 1977).

The entire group reaches a maximum thickness of 1400 meters in what is known as the Pasco Basin and consists of layered breccia, entablature, and colonnade units. There is a wide range in the physical properties of these basalt units as evidenced in many of the well log measurements. As an example, the average sonic velocity over any large section (on the order of 250 meters) is approximately 4.9 km/sec but this will contain breccia zones where the velocities are as low as 3.0 km/sec and as high as 6.8 km/sec in the colonnade (Lanning, 1981).

Although significant work has been carried out since 1969 in monitoring earthquake activity in eastern Washington (Malone, 1977), little use has been made of the boreholes at the Hanford site for active seismic investigations. The existence of the wells, and the fact that almost all VSP surveys have been done in marine sediment environments, provides an interesting research opportunity for studying in-situ attenuation using VSP measurements.

Description Of The Data

In July, 1983 a VSP survey was shot by a crew from the University of Wyoming by permission of the Department of Energy-Rockwell Operations on the Hanford Reservation. The uncased portion of a borehole, designated DC-7, from 869 to 1189 meters was selected for the experiment using a 3-component wall lock seismometer and approximately 8 meter receiver spacings. Figure IV-1 shows a sonic log taken over the portion of the borehole used for the survey where large variations in the sonic interval transit time can be seen. The VSP source consisted of two Bolt land airguns offset 152 meters from the well head on a gravel pad. During the survey the seismometer was locked into place at a particular down-hole position and twenty shots were recorded before moving to the next receiver depth.

Cavitation of the borehole walls was severe enough in several locations that it was impossible to lock the seismometer into place and these depths were then skipped during the survey. No recordings were made at four successive down-hole locations from 914 to 937 meters due to this difficulty although this was the largest gap in coverage.

Finally, the data were acquired at a sampling rate of 2 msec. I have indicated previously that some of the formation velocities are as high as 6.8 km/sec and that the receiver spacings are 8 meters. This implies that these data are undersampled since in some cases the seismic energy can travel further than the distance between two receiver positions in a single time sample interval.

Unlike the ARCO data, which contained recordings on monitor and down-hole seismometers for each of the shots in the survey, the twenty shots at each down-hole receiver position on the Hanford data were stacked (summed and averaged) prior to being received for this study and no monitor phone measurements were made available. This means we will be unable to correct the borehole measurements for the variations in the source wave field. Also, we will obtain only one estimate of the first break time and frequency spectrum rather than multiple estimates for them at each depth.

The stacked data from depths 945 and 1181 meters are shown on figures IV-2 and IV-3 where the resonance or coupling response of the horizontal components is apparent on both records. Although it is not as regular from shot to shot as it was on the ARCO data, this signal dominates the horizontals especially in the later portions of the traces. As was done previously, we will restrict our analysis to the vertical component only at each depth. Since the ratio of the source offset to the borehole receiver depth is less than 0.18 throughout the entire survey, the initial arrivals will all be very close to vertical and the loss of the horizontal components will have little effect on this study.

Data Reduction

Travel Times. Errors in the first arrival times for the Hanford VSP are apparent on the travel time data shown in figure IV-4. The measurements at both 991 and 1067 meters are significantly longer than those at nearby depths. In addition, the travel times beginning with depth 1052 meters appear to be delayed on the order of 10 msec with respect to the trend of the shallower data. There is nothing in the sonic log at 1052 meters that would indicate an increase in the travel time of this magnitude and since we are shooting at nearly

vertical incidence there is no physical way that the travel times at 991 and 1067 meters could be longer than those at lower depths. Either the arrival times were picked inaccurately or the delays are due to shifts in the data.

In figure IV-5 are sections of the vertical traces from depths of 889 (top), 1029 (middle), and 1189 (bottom) meters where the first break times are indicated on each graph. From these it can be seen that the accuracy of the time picks is quite good therefore the scatter in the travel time measurements on figure IV-4 is not due to an inability to determine the onset of the first arrivals but must be due to shifts in the data.

The zero or shot time of the seismic data is determined automatically by equipment in the field. A signal from an accelerometer attached directly to the source is fed through electronics that determines the time of first motion and delays the recording of all the data by this amount. Any errors in determining this recording delay will of course lead to an inaccurate zero time for that shot.

If there are shifts of one trace with respect to another at the same borehole depths then this would lead to improper stacking of the data for that depth and a distortion of the waveform. This is one possibility for the unusual appearance of the onset of the first arrival at 1189 meters. Rather than a definite break and decrease to the first minimum, there is a two stage progression in the beginning of the waveform.

Although nothing conclusive can be said concerning the possibility of time shifts in the records it does seem that the arrival times are well determined and that the scatter as well as the delay in the deeper travel times is not due to the first break analysis.

Frequency Spectra. Amplitude spectra were computed for the vertical component at each depth using the predictive deconvolution and spectral estimation techniques of Chapter III. The results from four widely spaced depths of the survey are shown on figure IV-6 and IV-7 over frequencies of 0 to 150 Hz. The frequency content varies radically from one spectrum to another where the one for the shallowest receiver position (869 meters) is at the top of figure IV-6. This is a clear indication that variations in the source during the

course of the survey are large enough that they cannot even be assumed to be approximately constant.

Without a constant source wavefield, or the monitor phone data to correct for the fluctuations, variations in the spectral ratios between two down-hole receiver positions are not due solely to the attenuation of the medium. In figures IV-6 and IV-7 we do not see a consistent decrease in high frequency content with increasing depth which we would expect if the source were the same for each record. This means we will be unable to make any attenuation estimates using the inverse method.

Drift Times. Using the sonic log data shown on figure IV-1 and the VSP travel times (converted to vertical) the two travel time curves shown on figure IV-8 were computed beginning at a depth of 867 meters. Once again the VSP travel times are longer than the sonic as we expect from the higher frequency waves. Subtracting the two curves to get the drift times, shown on figure IV-9, the offset in the VSP travel times that begins at 1052 meters is even more apparent, as are the anomalous times at 991 and 1067 meters. I will eliminate these last two measurements (those from 991 and 1067 meters) from the data set. The delays are so large that the travel times are unrelated to the ones at the surrounding depths. Before we can proceed with the attenuation estimate we must correct for the apparent delay of the measurements below 1052 meters. In order to estimate the magnitude of the offset between the shallow and deep section, we can make linear fits to the data over the portions of the drift time curve just before and just after the offset as shown in figure IV-10. The offset at the overlap of the two linear trends is found to be 8.75 msec. Let us now assume that this is the delay in the travel times of the deeper positions due to either recording or improper stacking procedures. Subtracting this 8.75 msec from all of the times corresponding to depths below 1052 meters results in the drift time dispersion curve shown in figure IV-11. Although there is considerable scatter in this data the trend is towards increasing drift times with increasing depth.

Attenuation Results -- Hanford Data

The scatter in the data is such that any structure in the attenuation profile is not apparent on the drift times. Using a center frequency of 30 Hz for the VSP data, 20 kHz as the sonic frequency, and an average sonic velocity of 4.87 km/sec, we can compute a linear fit over the entire drift time data set of figure IV-9 and calculate an estimate of the average attenuation of:

$$Q^{-1} = 0.015 \pm .005 .$$

These values imply that each frequency component of a propagating seismic wave would lose, on the average, between 6.25 and 13.5% of its energy per cycle in these basalt sequences.

This result is limited to a fairly narrow depth interval, roughly .8 to 1.2 km, and is an average over this range rather than being representative of any one of the types of basalt units (breccia, entablature or colonnade) that comprise the formations adjacent to the borehole. The quality of the travel times was not as good as with the ARCO data set and resulted in a lack of any structural interpretation of the data. This is due in part to the slow sampling rate (2 msec rather than at least 1 msec) but also to what appears to be related to a miscalculation in the zero time for some of the shots in the survey and a shift in this same time for others. Whether these took place at acquisition time, in the stacking procedure, or both is not clear from this analysis.

Conclusion

The analysis of the Hanford VSP, and the difficulties encountered, makes it apparent that care must be taken during the acquisition phase of the experiment and the processing of the data if usable information is to be obtained. Some of the problems encountered and suggestions for avoiding them are listed below.

1.) Sampling Rate

The geophone spacing of 8 meters was a good idea since the sonic log shown on figure

IV-1 indicates there exists significant fine scale structure but a sampling rate of 2 msec is too slow given the velocities implied by the logging data. Ideally, the data should be taken at as high a rate as possible, since this would allow the greatest resolution for timing arrivals, but this rate is usually limited by the acquisition system. At any rate, 1 msec sampling rates are available with most field systems and would have been more appropriate for this survey.

2.) Determining Zero Time

In general this should not be a problem on a VSP experiment. Most equipment used for this purpose is reliable and consistent but we saw clear evidence for shifts or time delays from one depth to another. While this could have occurred at the time the data was stacked, this would represent a gross error on the part of the processor. The alternative to using automated equipment for determining the source time is to record the shot geophone (in this case the accelerometer) and establish zero times for each shot record at the early processing stage of the analysis.

3.) Monitor Phone Recordings

The results for the Hanford data demonstrate that these are a necessity for computing spectral ratio slopes that contain information about the attenuation structure. Without the monitor data we have no way of ascertaining if the source was stable during the survey or correcting for variations if it was not. On site processing of the monitor phone records could even be used to indicate when the source variations are becoming so large as to make it necessary to alter the progress of the experiment (i.e. move the source to a new location, check for faulty equipment, etc.).

4.) Stacking

For the purposes of computing attenuation, leaving the data in a single shot format is best. This allows for multiple determinations of the travel time and spectral ratio slope at each depth which can be combined to get statistically more reliable values. Even if the data were to be stacked, the source variations must be removed first using

the monitor phone recording. Cross-correlations could then be used to determine if there are any time shifts of one trace with respect to another.

Finally, as in any experiment, it is necessary to pay careful attention to the proper functioning and operation of all equipment involved with VSP data acquisition and the subsequent processing. As was the case in this experiment, lack of this attention severely impacts the analysis and degrades the quality of the results that would otherwise be possible.

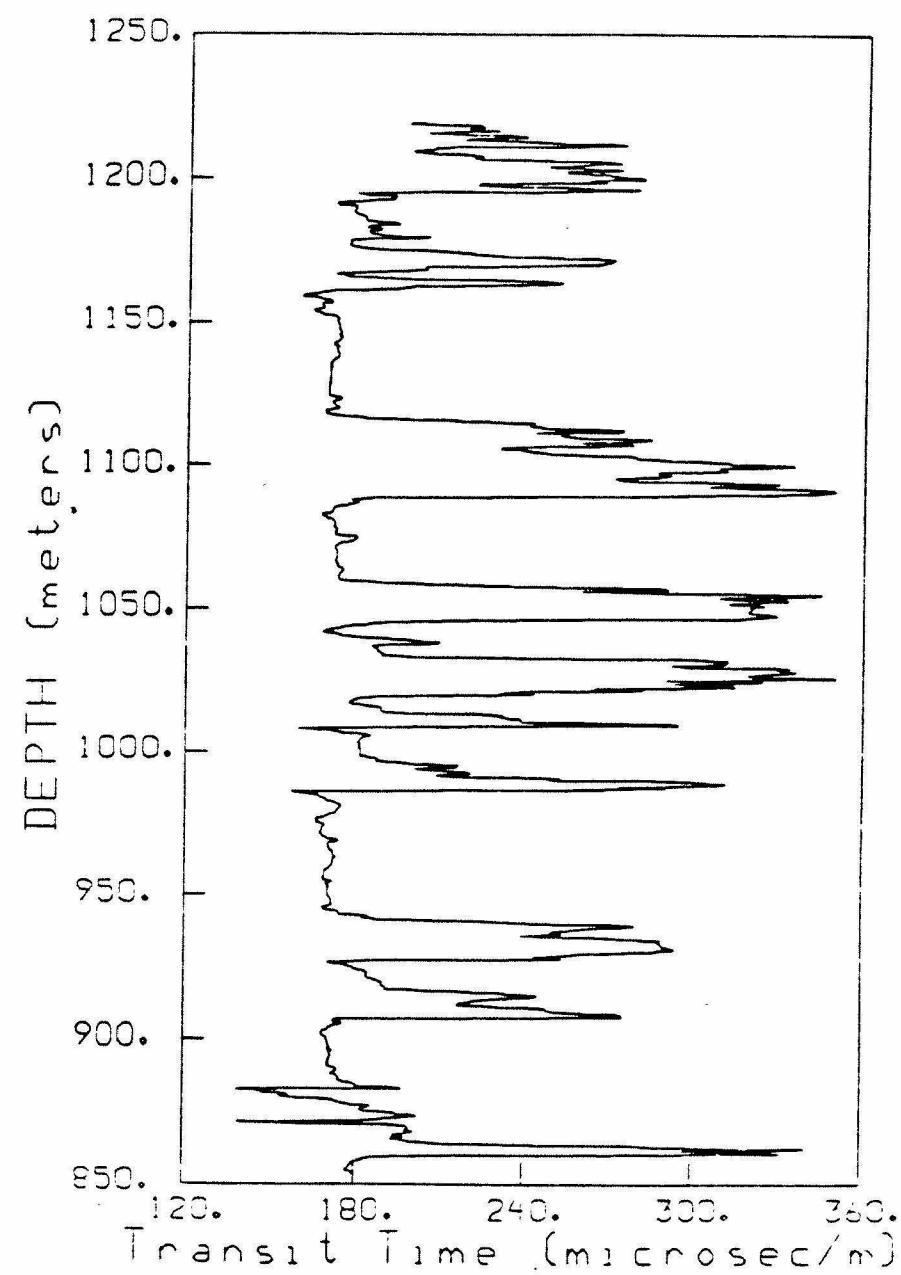


Figure IV-1. Sonic log taken from borehole DC-7 on the Hanford Nuclear Reservation covering the depth range of the VSP experiment.

RECD DEPTH (meters) - 945.

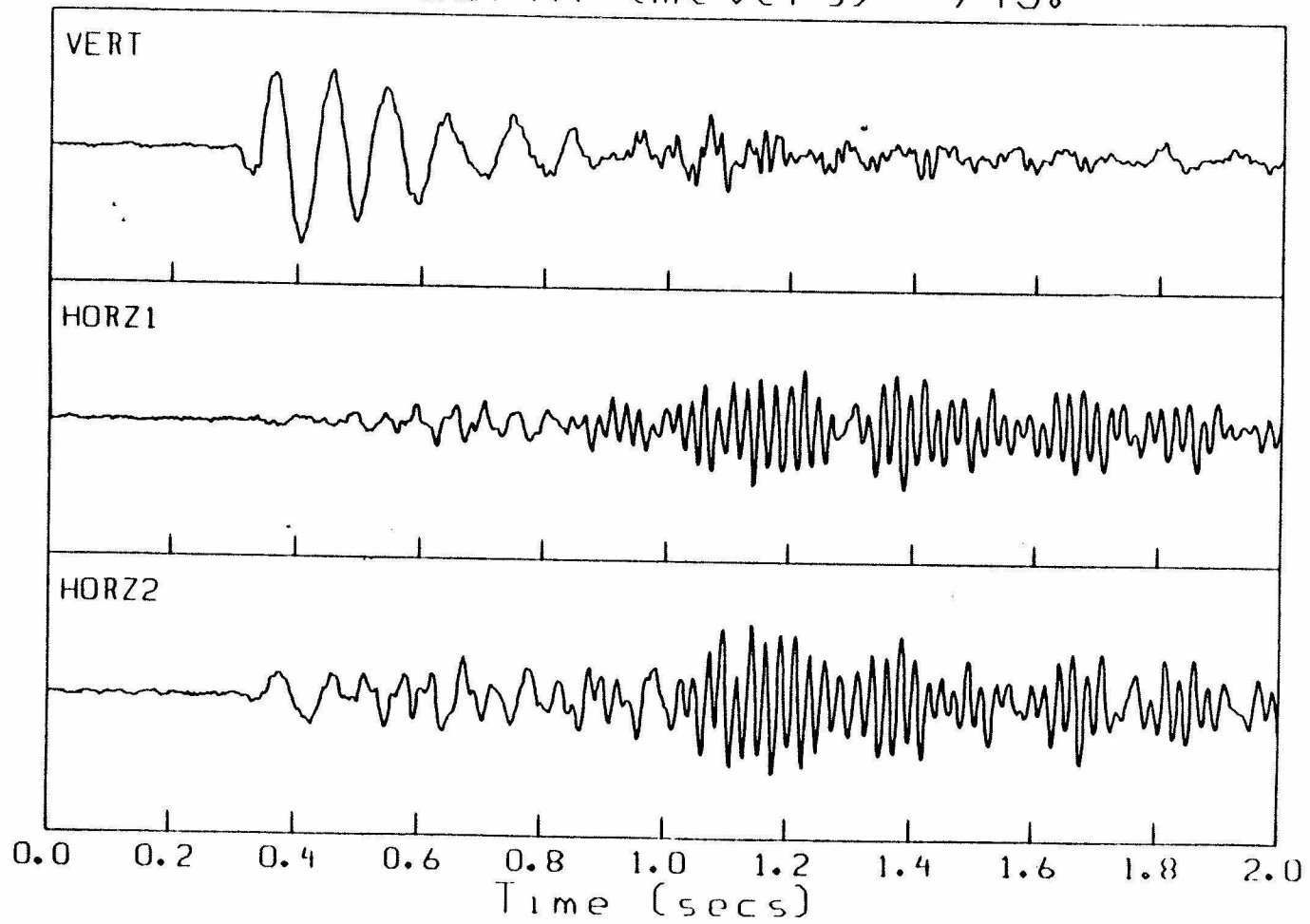


Figure IV-2. Three component seismic record of the stacked data from a borehole depth of 945 meters. The plotting amplitudes are equal on all three channels.

RECD DEPTH (meters) - 1181.

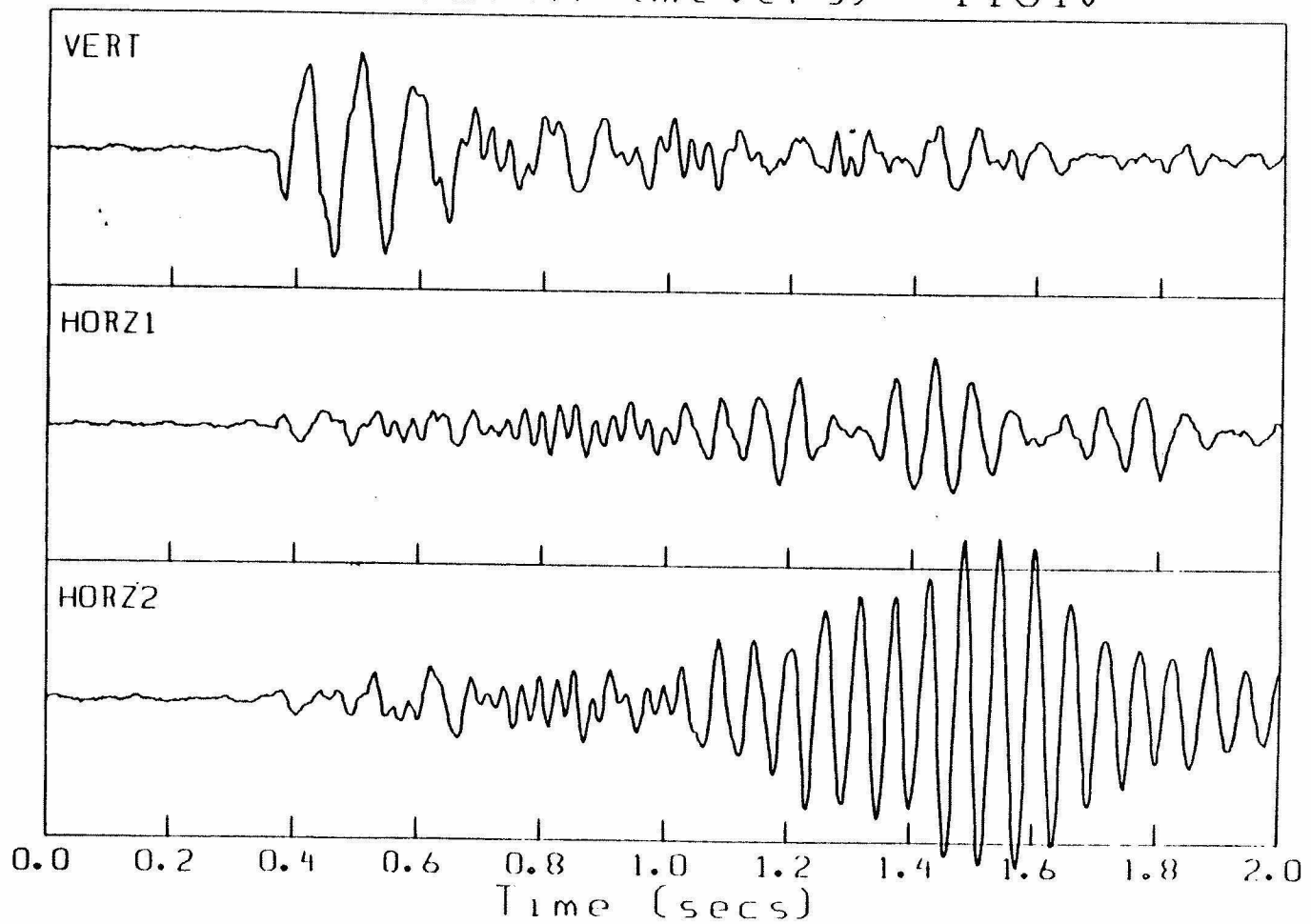


Figure IV-3. Three component seismic record of the stacked data from a borehole depth of 1181 meters. The plotting amplitudes are equal on all three channels.

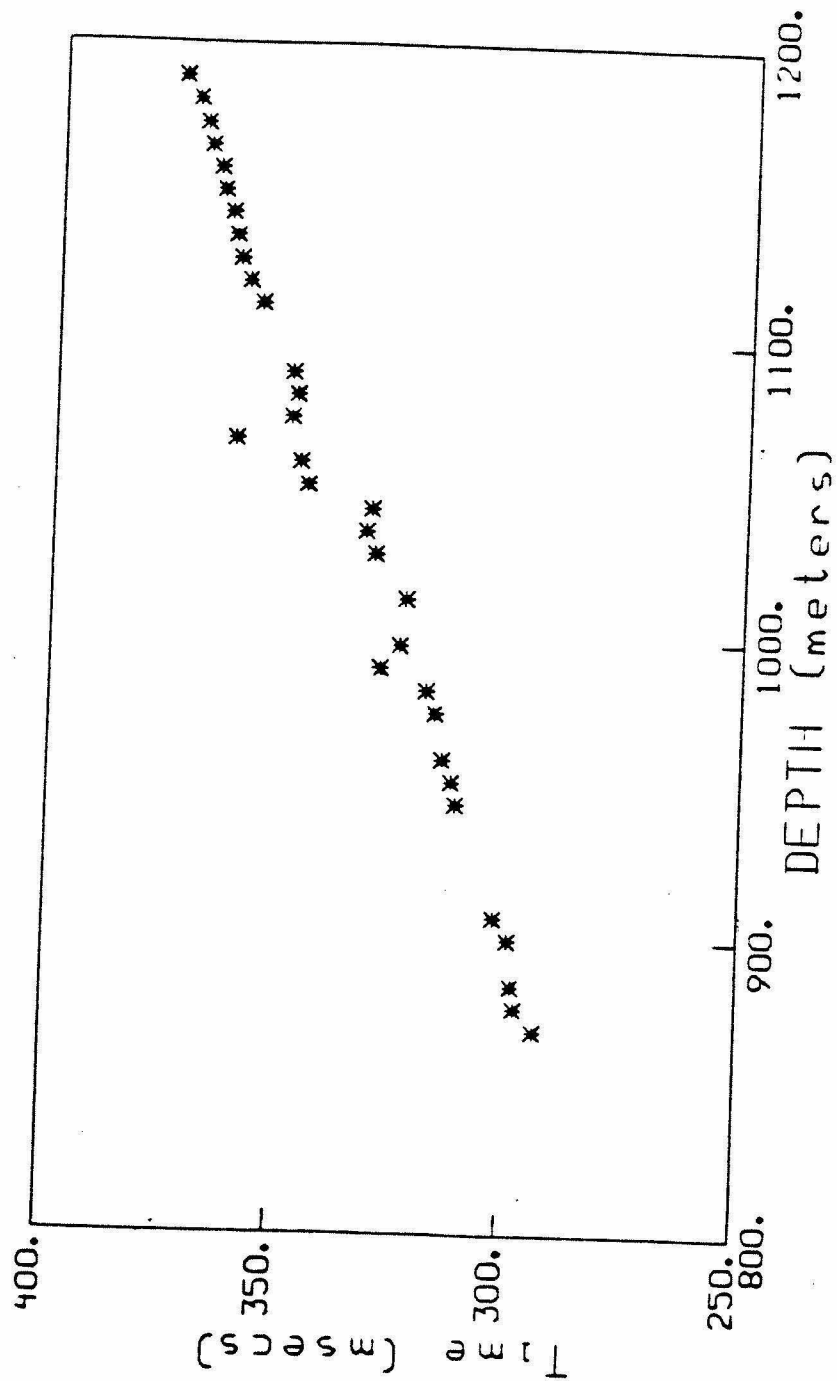


Figure IV-4. The first arrival times are shown for the Hanford VSP data set. The gaps in the data are due to an inability to lock the seismometer into the borehole at those depths.

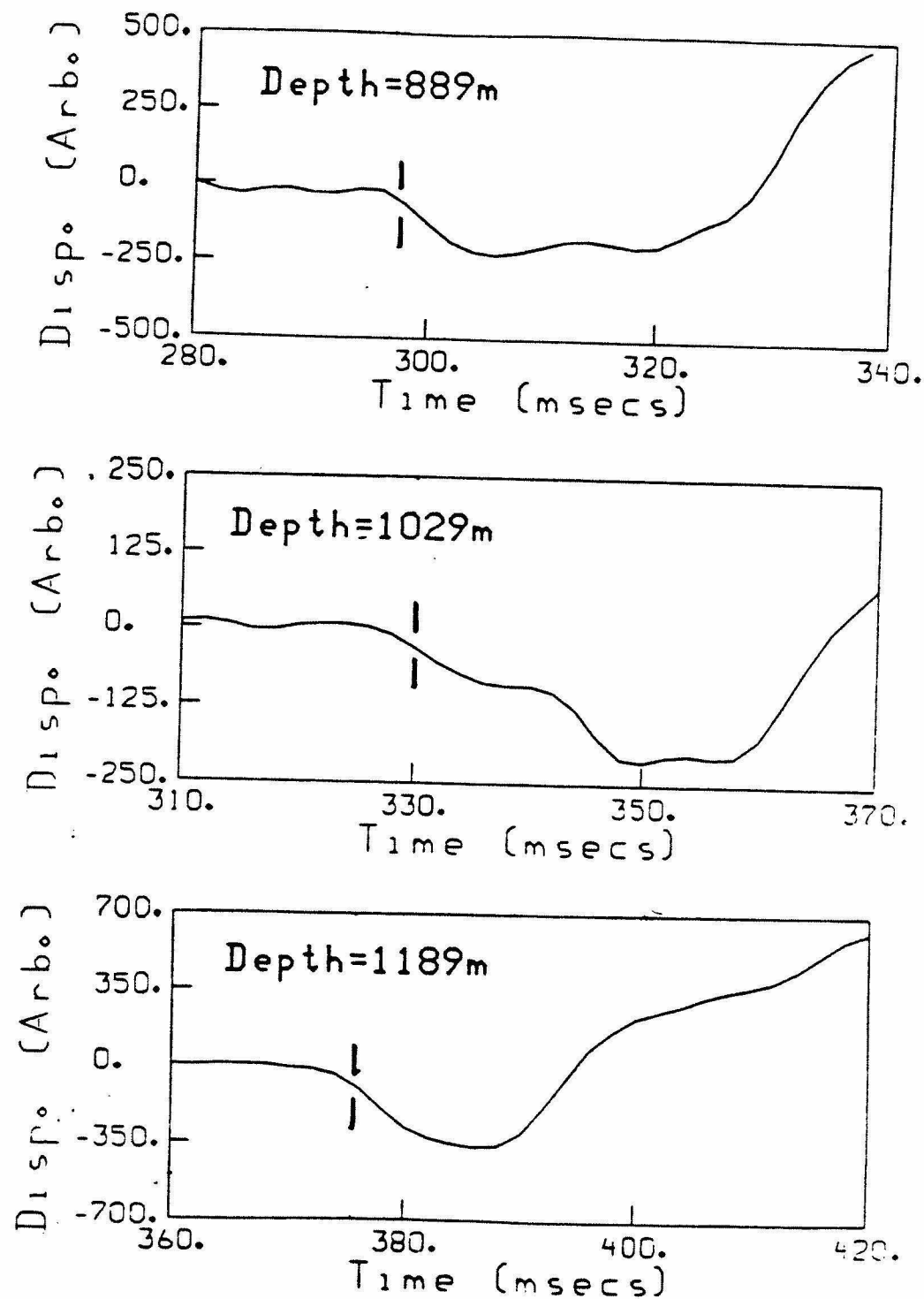


Figure IV-5. Sections of the vertical component traces from depths of 889 (top), 1029 (middle), and 1189 (bottom) meters of the Hanford VSP data. The first arrival times are indicated on each graph by the vertical dashes.

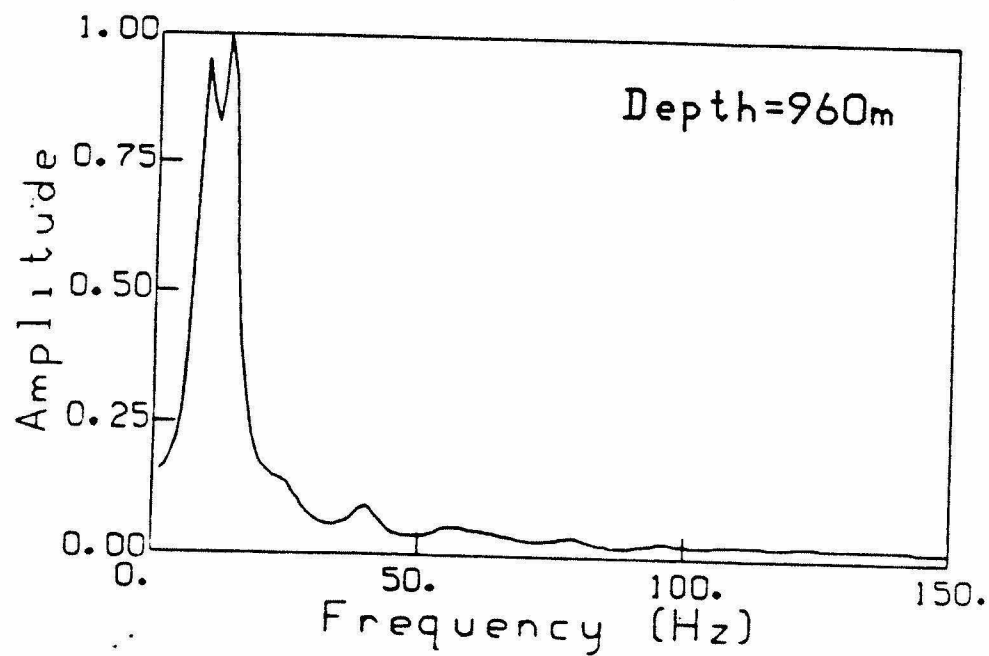
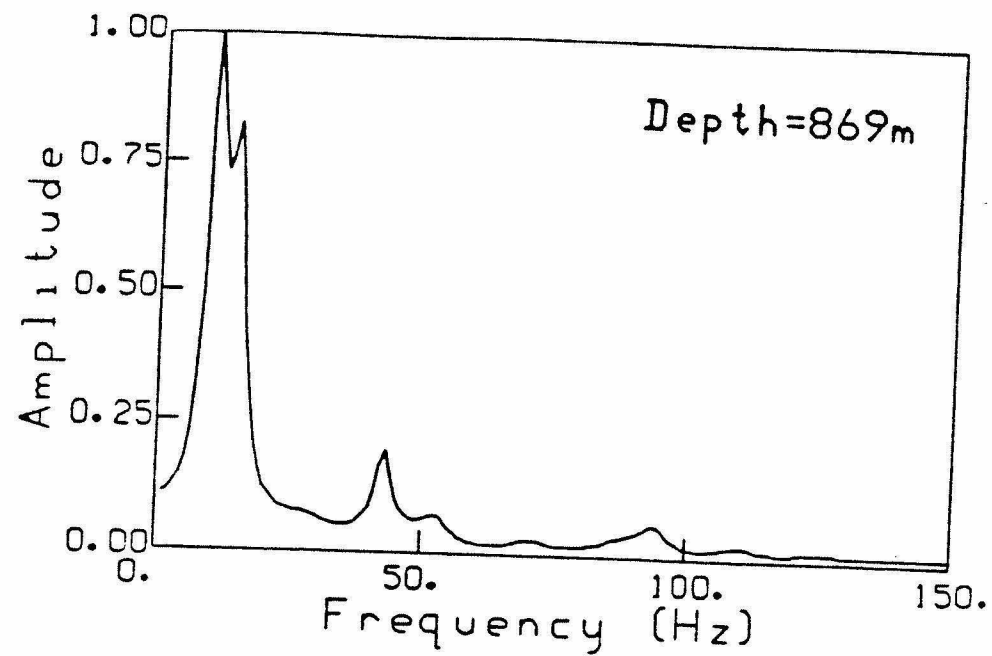


Figure IV-6. Frequency spectra using an approximately 144 msec. time window beginning with the first arrival times for depths 869 (top) and 960 (bottom) meters.

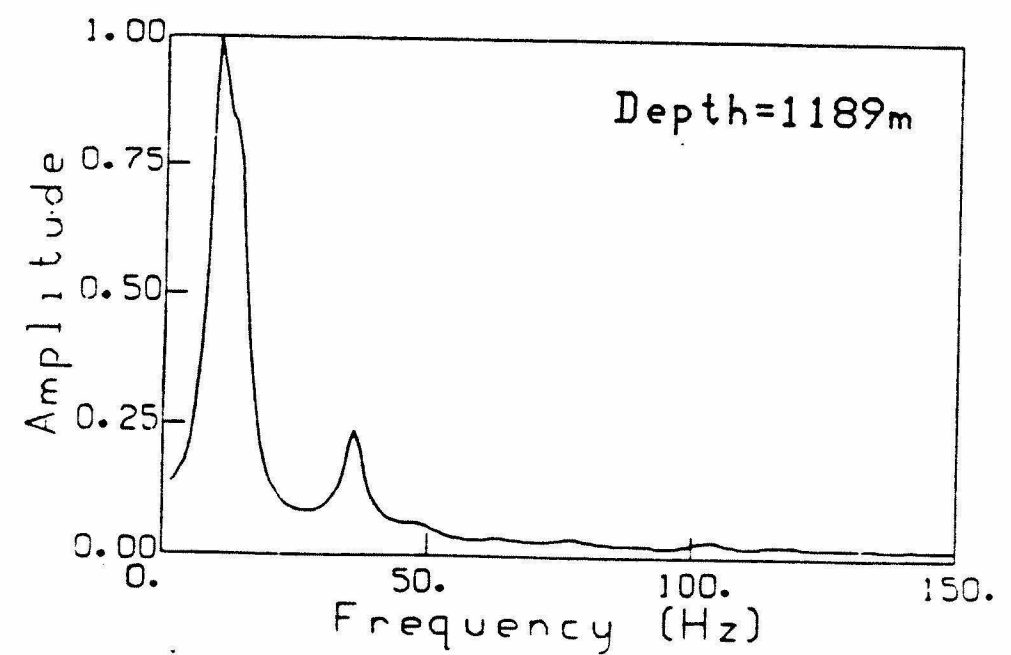
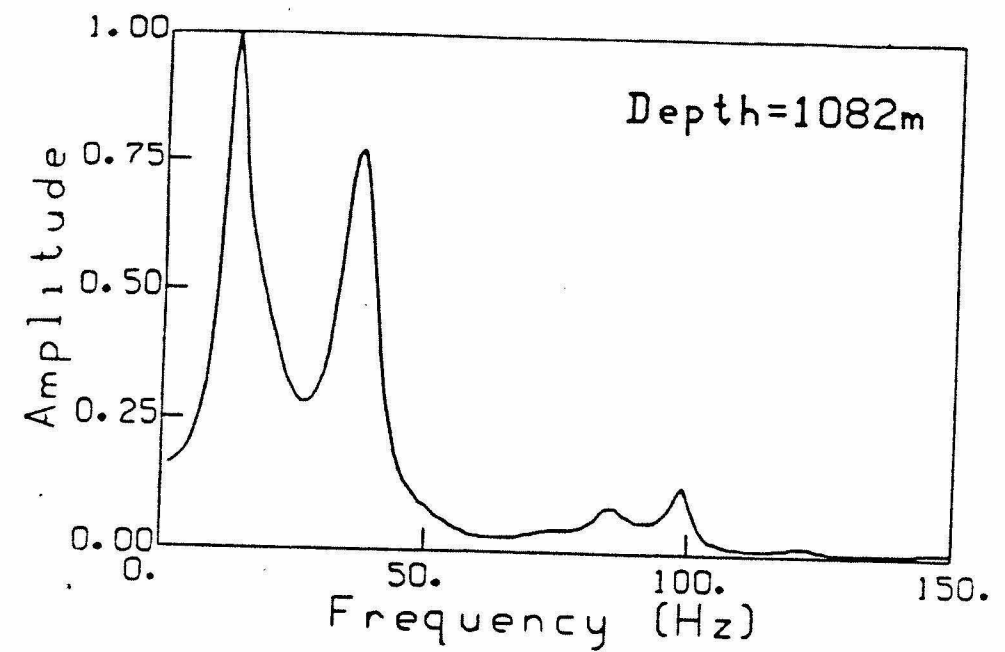


Figure IV-7. Frequency spectra using an approximately 144 msec. time window beginning with the first arrival times for depths 1082 (top) and 1189 (bottom) meters.

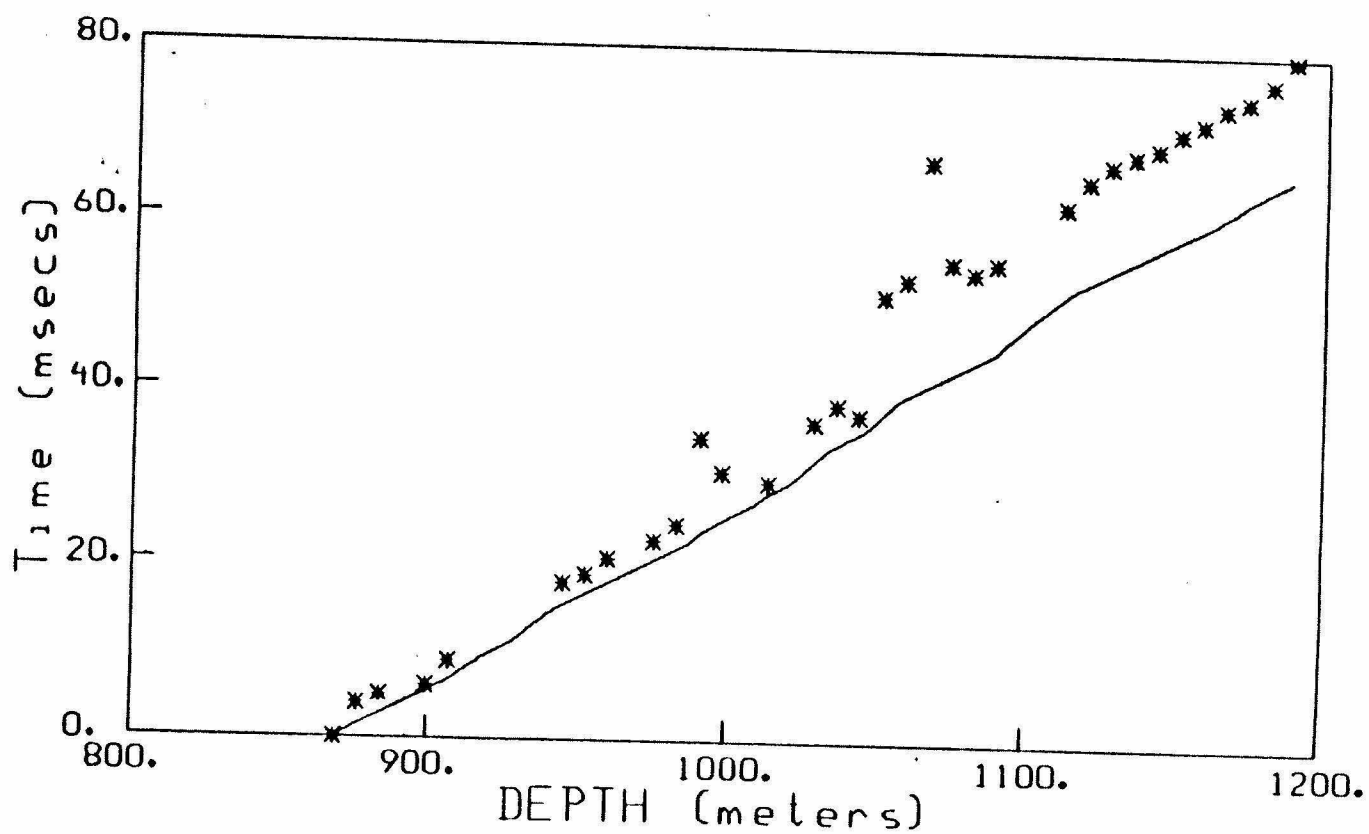


Figure IV-8. The asterisks are the Hanford VSP travel times converted to vertical after having subtracted the vertical time down to 860 meters from each of the deeper measurements. The solid line is the integrated sonic log, shown in figure 7-1, beginning from a depth of 860 meters.

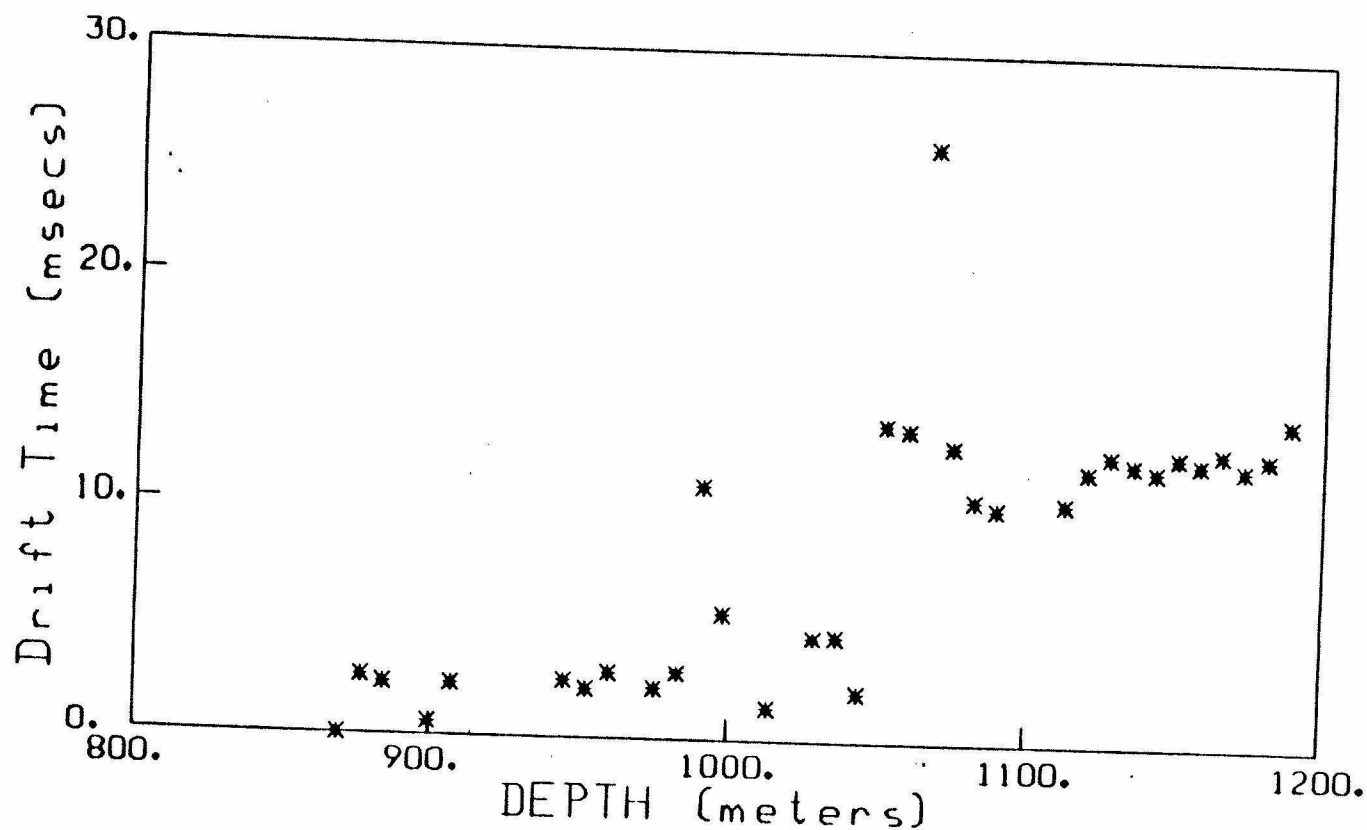


Figure IV-9. Drift time curve for the Hanford VSP computed by subtracting the two curves shown in figure 7-8. Note the apparent offset in the deeper measurements beginning with the data at 1052 meters.

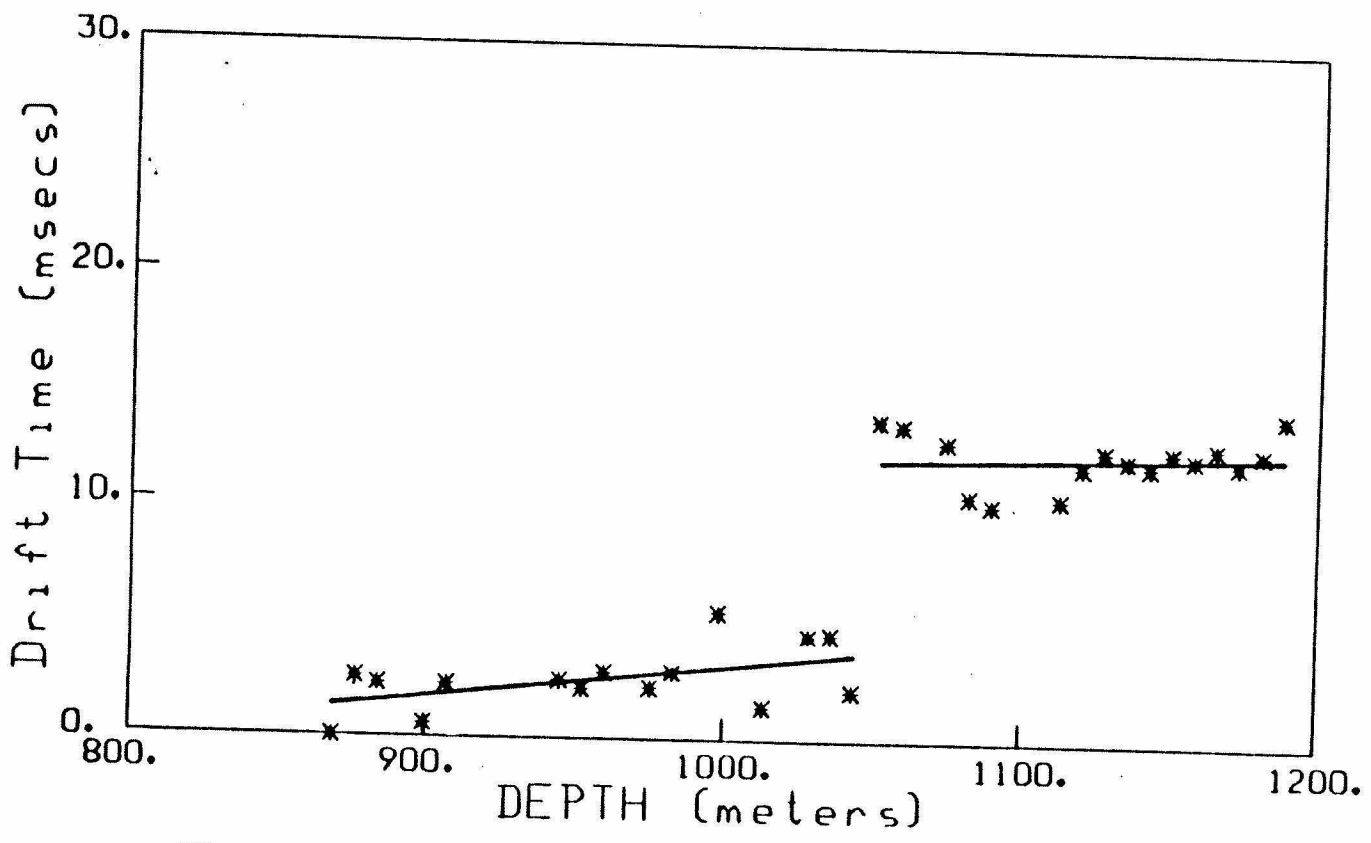


Figure IV-10. Linear fits are shown over the shallow (before the offset at 1052 meters) and the deeper portions of the drift time data. The two outlying points at 901 and 1087 meters were deleted from the data set prior to the linear regression.

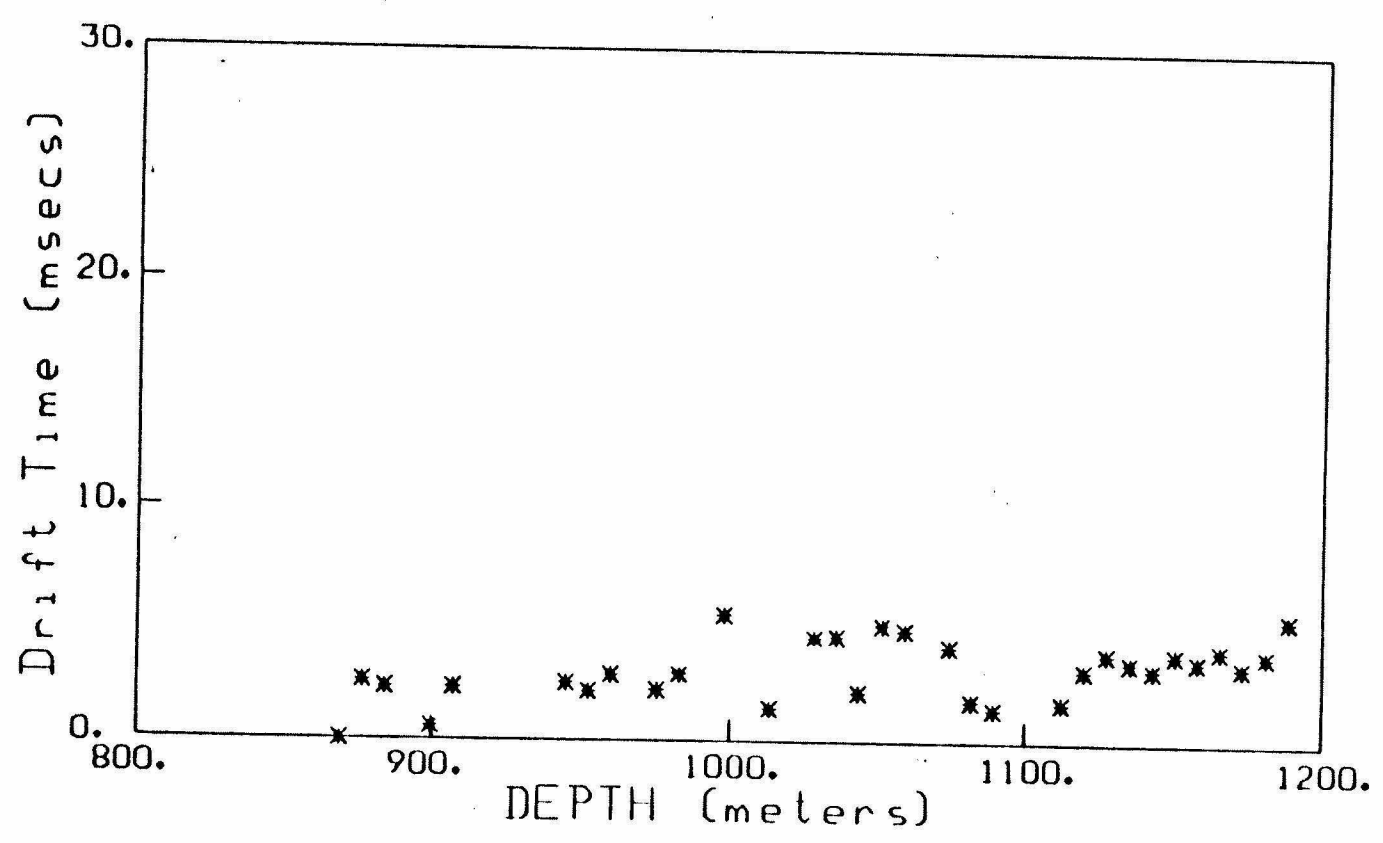


Figure IV-11. The drift time dispersion curve for the Hanford VSP after subtracting the computed 8.75 msec offset from the data points below 1052 meters.

SPECIAL STUDIES

Several individual special studies have been initiated over the past year that have applicability to the seismicity or tectonics of eastern Washington. These include a study of an earthquake swarm near Vantage, Washington, a study of an unusual earthquake sequence in eastern Oregon near the site of the Powder River landslide, and a study of high precision earthquake relocation technique which has been tested on a sequence of construction blasts in south eastern Washington.

Vantage Earthquake Swarm

In October, 1984 a sequence of earthquakes began 12 km northwest of Vantage, Washington, near the intersection of Highway 90 and the Columbia River (Figure I-4). Through June, 1985, 26 earthquakes between magnitudes 1.3 and 3.3 were recorded. At the time of this writing (September, 1985) several more have occurred. Depths are poorly controlled because the earthquakes are shallow and our nearest station is at a distance of 12 km. Precise epicenters are difficult to obtain because Vantage is near the boundary of two velocity models. However, the use of several combinations of velocity models and station corrections indicate that the spatial limits of the cluster of epicenters is well determined; only the depths vary significantly and nearly half of the events are fixed at a shallow depth by the computer algorithm. Characteristics of the waveforms and comparison of this swarm with others in eastern Washington lead us to conclude that these events most likely occurred at a depth of 1.0 km \pm 0.5. Focal mechanism plots are fairly well determined and indicate thrust faulting with an east-northeast axis. There appears to be no trend of earthquake magnitude or position with time. This is consistent with most other swarms in eastern Washington. The b-value for this swarm is 0.8. The minimum magnitude above which our data base is complete is $M=2.1$.

Locations

Obtaining precise locations of the Vantage earthquakes is difficult because this area is

near the boundary of two velocity models. The earthquakes were originally located with the northeastern Washington velocity model N3 (Table V-1). This model was modified for the Vantage area based on the study of borehole and refraction data from the Columbia Basin by Mr. David Glover (Master's Thesis, 1985). Station corrections were obtained for the modified N3 model by the master event technique, using the Whiskey Dick blast of June, 1981 as the master event. Stations beyond 90 km were not used with either model.

Locations of the earthquakes using the N3 and modified velocity models are shown in Figure V-1. The average difference in epicentral location between the two models is approximately 1.5 km. However, the distribution of epicenters for both models is in nearly the same, 4 km by 10 km area. Depths vary more significantly and are not considered accurate for either model. This poor depth control is due to the shallow nature of the earthquakes and lack of station coverage in the immediate swarm area.

Standard N3 model		Modified model	
P Velocity (km/s)	Depth to Top of Layer (km)	P Velocity (km/s)	Depth to Top of Layer (km)
5.1	0.0	3.7	0.0
6.1	0.5	4.9	0.5
6.4	14.0	6.2	4.4
7.1	24.0	7.2	22.5
7.9	38.0	7.9	37.0

The low frequency content of the waveforms and the ratio of body to surface wave amplitudes along with the knowledge that most eastern Washington swarms occur at a depth of 1.0 km \pm 0.5, lead us to believe the depths of the earthquakes in this study cluster around 1.0 km. With this in mind, the 26 earthquakes were relocated with the modified velocity model, holding the depths fixed at 1.0 km. This only moved the epicenters (Figure V-2) an average amount of approximately 0.3 km and further indicates that the epicenters are well determined.

Fault Plane Solutions

The fault plane solution of the largest event indicates thrust faulting. A composite focal mechanism solution of the seven largest events (Figure V-3) further constrains the solution, although there are several inconsistencies. Takeoff angles were calculated using a linear gradient with an initial velocity of 4.2 km/s and a gradient of 0.08 km/s/km. First motion data are plotted using an upper hemisphere, equal area projection. The composite solution shows a predominantly thrust mechanism with nodal planes striking N68E and N90E and a maximum compressive stress direction of S20E. This mechanism is very similar to the 14 November 1983 $M=3.8$ Yakima event (see *Annual Technical Report, 1984*), and is consistent with other events in eastern Washington, *ie*, events in the Lake Chelan area (see *Annual Technical Report, 1978*), and the Wahluke, Eltopia, and Royal swarms of 1972-74. Projections of the hypocenters onto vertical planes perpendicular to those of the composite focal mechanism do not reveal a preferred plane along which the earthquakes lie.

Time and Magnitude Distribution

Time distribution studies were applied to the 26 Vantage earthquakes. There was no obvious trend of magnitude with time. This sequence of earthquakes occurred as a swarm with a gradual increase and subsequent decrease in seismic activity, with no one event large enough to be considered a main shock. This is characteristic of most of the eastern Washington seismicity. Depth, latitude, and longitude were also plotted versus time, and no spatial migration with time was found.

The b-value for this swarm of earthquakes was calculated using the linear relationship

$$\log N = A - bM$$

where N is the number of earthquakes greater than or equal to the magnitude M . Figure V-4 shows the graph of $\log N$ vs. magnitude. The line of best fit yields a b-value of 0.8 above $M=2.1$. Below $M=2.1$, there appears to be a drop in the slope. This may indicate that at these lower magnitudes, we were not detecting all the events. This seems reason-

able because if more than one critical station is down, the earthquake probably would not be detected by our computer detection system.

The Powder River, Oregon Earthquakes of 1984

by J. Zollweg and R. Jacobson (Oregon State University)

(Condensation of paper in preparation for submission to BSSA)

Introduction

On 18 September 1984 a major landslide occurred in the Wallowa Mountains region of northeastern Oregon. The landslide dammed the Powder River, blocked Oregon Highway 86 and cut off normal communications with the communities of Halfway and Richland, Oregon (Figure V-5). Magnitude 3.8 earthquakes were felt in these towns on 10 August and 19 September 1984 UTC (10 August and 18 September PDT). Preliminary locations for these earthquakes computed by the National Earthquake Information Service (NEIS) and the University of Washington (UW) were of low quality, but suggested that the seismic activity could have occurred close to the landslide. To investigate the question of a connection between the earthquakes and the landslide, we deployed 5 portable seismographs in an effort to record and accurately locate aftershocks of the magnitude 3.8 events. This study was part of a broader geological and geophysical investigation of the landslide (Jacobson *et al.*, 1985). While that investigation cast strong doubt upon the possibility that there was any link between the landslide and earthquake activity, it nevertheless provided a rare opportunity to obtain detailed information on an eastern Oregon earthquake sequence.

Faulting in northeastern Oregon and adjacent portions of Idaho is extensive and complex. Several fault-bounded basins exist within the Blue and Wallowa Mountains. The 1984 earthquake sequence occurred in the vicinity of Pine Valley, which is surrounded by a complex system of faults (Ross, 1938; Brooks *et al.*, 1976). Those that bound the valley to the west and southwest have some expression in free air gravity anomalies (Berg, 1967). We are not aware of any attempts to date the most recent movements along the known

faults, but those that displace Columbia River Basalts are certainly post-Miocene and are probably much more recent.

Northeastern Oregon is certainly not renowned for its rate of seismic activity, but a search of available catalogs (Berg and Baker, 1963; Couch and Lowell, 1971) yielded 13 events within 50 km of Richland prior to 1981. Most earthquakes prior to 1962 were located from intensity data. Possibly the strongest shock on record as having occurred near Richland is that of 1916, which was of intensity VII. There is some uncertainty about the epicenter of this earthquake. The greatest damage (fallen chimneys) was reported from Boise, Idaho. We believe the epicenter was probably in Idaho rather than Oregon, although it may still have been within 50 km of Richland. The maximum intensity of all other known events has not exceeded V. Most of the smaller events were reported only from the Richland-Halfway area.

Main Shock Sequences

The first locatable earthquake within 50 km of Richland in 14 years occurred at 0539 UTC on 29 September 1981. It had a magnitude of 3.6 M_L and was felt at Cambridge, Idaho.

The next earthquake occurred at 0136 UTC on 29 March 1983. It had a magnitude of 3.4 M_L and was felt at Halfway. Numerous aftershocks were identified on seismograms of the Boise State University seismograph network, but none were reported felt nor could any be located. The duration of the aftershock sequence is unknown.

On 10 August 1984 at 0726 UTC, a magnitude 3.8 M_L earthquake occurred, preceded by a magnitude 2.7 event at 0751 UTC on 9 August and magnitude 2.8 events at 0337 UTC and 0614 UTC on 10 August. No aftershocks were recorded on regional stations, whose detection threshold is estimated at 2.5 M_L . Only the main shock was reported felt. Most reports of this quake came from the Richland-Halfway area; maximum intensity was probably IV MM.

On 19 September 1984 at 0132 UTC, a second magnitude 3.8 M_L shock occurred and was felt at Halfway and Richland with intensities similar to the 10 August event. Neither foreshocks nor aftershocks were recorded on regional stations.

A version of HYPOINVERSE (Klein, 1978) was used to locate the 4 largest regionally-recorded events between 1981 and 1984. We used the Northern Nevada/Southern Idaho (NNSI) model of Hill and Pakiser (1966) to calculate travel times to regional stations, except for one station near Boise for which Hill and Pakiser's Western Snake River Plain model seemed more appropriate. Stations in the interior of the Columbia Plateau or beyond a distance of about 400 km were not used. These restrictions insure that the stations used are situated upon somewhat similar crust. Our version of HYPOINVERSE calculates surface elevation corrections and 95% confidence ellipses. Results of these computations are shown in Figure V-6. Formal uncertainties are large. For the 1983 event the major horizontal axis of the 95% confidence ellipsoid has a half length of about 5 km, which roughly corresponds to the expected location accuracy. For the 1981 earthquake and the two 1984 events the half-length is about 20 - 30 km; moreover these solutions would not converge unless the computation was started somewhere in the Halfway region. In the absence of detailed knowledge of velocity models and station corrections, the calculated uncertainties are underestimates of the errors to be found in the regional locations.

While we were unable to calculate accurate epicenters for any of the larger events, we were able to glean some information from inspection of waveforms recorded on stations of the UW network. These stations are recorded digitally with sampling frequencies of 100 Hz, so rather fine resolution exists for the frequencies less than 4 Hz which predominate on recordings of the main shocks. The distance to the nearest station was about 170 km. While only a few stations recorded all 4 events and the comparisons are complicated by noise, we found that waveforms for the two magnitude 3.8 events of 1984 were essentially identical in the *S* and surface wave portions of the seismograms. The *P*-wave portions are less coherent. Recordings of the 1981 and 1983 earthquakes are somewhat similar to each

other, but share only very general characteristics with the 1984 shocks. $S-P$ intervals seem to be a little shorter for the 1984 quakes, indicating sources slightly north or west of the earlier events. Overall, the recordings of the 1984 earthquakes are so similar as to suggest sources within 1 or 2 km of each other. We suggest that the 1983 hypocenter is perhaps 5 km away in a southerly or easterly direction. The 1981 earthquake is probably 10 km or so east of the 1984 epicenters. The important conclusion is that all the larger events recorded regionally come from a relatively small source area.

Microearthquake Studies

Since the 1984 earthquakes were felt most strongly in the Richland- Halfway area, we centered our network of 5 portable stations upon these communities. Recording with as many as 5 stations was maintained from 3 to 7 October 1984. 34 tectonic earthquakes with $S-P$ intervals less than 4 sec on the closest station were identified on the network records. Phases of 15 events were recorded on 3 or more stations. We calculate magnitudes (M_L) of -0.8 to 1.8 for these events.

We calculated hypocenters using a crustal model somewhat similar to the NNSI model. Our layer velocities are generally lower and were estimated from apparent velocities of phases of regional earthquakes recorded on the portable net. Experimentation with different velocity models indicates that the overall results are not particularly model-dependent.

For the P_n phase of a regional earthquake that occurred about 250 km to the east, temporary network data show a high apparent velocity of 9.1 ± 1.0 km/sec. While the lower limit is not an unreasonable P_n velocity, our data probably should be interpreted as indicating a eastward-dipping Moho exists under the portable network. This is consistent with the refraction studies of Hill (1972) and Hill and Pakiser (1966), which suggest the crust generally thins as one goes northwestward from the Basin and Range/Western Snake River Plain toward the Columbia Plateau. The dipping interface on the Moho does not affect our local network locations, since all events proved to be upper crustal in depth.

While we did not succeed in establishing very good azimuthal control on the events, the better locations tend to cluster strongly in 3 areas that are too far apart for the differences to be due to hypocentral uncertainties (Figure V-6). More importantly, each of the 3 clusters of events in Figure V-6 corresponds to an easily-recognized "characteristic signature" at stations of the portable network, chiefly distinguished by the move-out times between the 2 closest stations and their $S-P$ intervals. We are therefore confident of the relative distribution of the better-located events in Figure V-6. Focal depths are generally between 6 and 11 km.

Fault-Plane Solution

The main shocks of 1981-1984 were not sufficiently well-recorded at regional stations to allow determination of fault-plane solutions. Azimuthal control was poor, and very few unambiguous first-arrivals were recorded. The small number of stations in the portable network prevented single-event fault-plane solutions for any of the recorded aftershocks. Figure V-7 shows a composite using portable network data. Polarities could not be assigned with confidence to the majority of the local network recordings. Those we have plotted represent only the better first-motions. We also plotted the best regional data for the main shocks of 1983 and 1984. The composite is interpreted as indicating nearly pure normal faulting on a plane striking either N30W or N.

Conclusions

We have identified a small seismic zone near the mouth of Oregon's Powder River, which has been the locus of 4 earthquakes (M_L 3.4 - 3.8) since 1981 and about 10 other events of comparable magnitude since 1915. Activity extends across the Snake River into Idaho, based on both intensity and instrumental data.

Microearthquake monitoring subsequent to M_L 3.8 events in 1984 resulted in identification of the source region of the larger events near Pine Valley. A composite fault-plane solution is evidence for continuation of the Basin and Range extensional stress field

into northeast Oregon. There was no apparent connection between the earthquake activity and a major landslide along the Powder River which occurred on 18 September 1984.

Recordings of regional earthquakes on the portable stations indicate that crustal structure is similar to that interpreted for northern Nevada and southwestern Idaho (exclusive of the western Snake River Plain). A high apparent P_n velocity is probably indicative of crustal thinning in a westward direction.

Precise Relative Location Procedure

Section from a paper in preparation

by M. Fremont and S. Malone

Introduction

We have been working on a new technique for locating earthquakes relative to one another with very high precision. This technique was first proposed by a group of researchers in Grenoble, France led by George Popinet. His student, Marie-jo Fremont has been working with us for the past year on various applications of this technique and has applied it to both volcanic earthquakes at Mount St. Helens as well as a series of construction blasts in eastern Washington.

The technique involves computing the cross-spectrum of a short time window of the P-wave of two events with very similar wave-form. The slope of the phase of this spectrum is proportional to the arrival time difference between the two stations. The precision of determining this arrival time difference can be as high as one millisecond, even for data sampled only every ten milliseconds. Given precise arrival-time differences at several different stations and knowing the direction that each wave pair takes to get to each station one can easily compute the position of one event relative to the other. This procedure has been tested using a sequence of blasts near Ice Harbor Dam. The results are given in the rest of this section which is an excerpt from a paper describing the technique and application to data from Mount St. Helens. The techniques applicability to swarm events in

eastern Washington has not been tested yet but will be investigated during the coming year.

The data we used were from a project for a navigation channel improvement in Eastern Washington. Twenty-three explosions which occurred during a one-week period have been studied as a multiplet. They were recorded at several stations in a distance range from 22 to 120 km. Examples of seismograms are shown in figure V-8. The reference event of this multiplet is the explosion which occurred on February 20 at 22:34. Distances between actual positions of an explosion of the sequence and the reference explosion chosen were in the range of a few meters to about 350 m. Each explosion was actually a linear distribution of charges about 50m long. We arbitrarily chose the hypocenters of the actual positions as the middle of each line of charges. The coda duration magnitude of the explosions is about 1.0 (the mean weight of explosive charges is about 1000 pounds). The size of the events as well as the medium encountered affect the signal to noise ratios. They do not affect the relocation process since we compare multiplet events with similar sizes. Nevertheless, large magnitude earthquakes will lead to better relocations because of higher signal to noise ratios and larger number of usable stations. In order to test the limits of the method we used a small number of stations, 7 or 8, distributed in different azimuths. Differences in P-arrival times, dt , have been computed in the frequency band 3 - 15 Hz which approximately represents the frequency content of these events.

Because of the station distribution (no station close to the epicenter) it was not possible to relocate the explosions in 3 dimensions. Indeed the decomposition in singular values cannot be done because of insufficient data. Therefore the explosions have been relocated in 2 dimensions (epicenter only) by fixing their depth which is a realistic assumption since the explosions occurred at the same depth. We considered a P velocity V_P in the source region of 4.2 km/s, a value appropriate for a shallow basalt structure. Also, $V_P = 4.2$ km/s minimizes differences between the positions obtained by the relocation technique and the actual positions.

The comparison of computed and actual epicenters of explosions are presented in figure V-9. The agreement between computed and actual epicenters is very good. Differences are generally of a few meters and always less than 25 m. In part, this may be due to the simplification of considering explosions as point sources (each explosion occurred along a line of about 50 m). This is unrealistic but similar to the representation of natural microearthquakes. On the other hand, we assumed in the computation that no change occurred in the data acquisition process during this one week period. The lack of correlation between differences in positions and time intervals separating the explosions and the reference event does not seem to contradict this hypothesis. The 19 explosions which were less than 250 m from the reference event were relocated with errors less than 25 m. The 3 explosions which were about 350 m from that reference event had grossly erroneous locations (greater than 350 m). This distance of 350 m is above a quarter wavelength for these explosions ($50 \text{ m} < \lambda / 4 < 250 \text{ m}$). $\lambda / 4$ as mentioned by several authors [*Geller and Mueller, 1980 ; Frankel, 1982a ; Pechmann and Kanamori, 1982*] seems to be the natural limit above which waveforms are too different to constitute a doublet and thus to allow for the relative location of the events using this technique.

In summary, this test on explosions data provides 2 important results as regards the relocation method of earthquakes within a multiplet:

- first of all, the agreement between computed and actual locations of explosions proves that this technique is quite valid even in poor conditions of low signal to noise ratios and station distribution.
- differences obtained between the positions give an estimation of the precision of the method. In this example the maximal error bar was 25 m. This dimension depends on V_P assumed in the source region which was here 4.2 km/s.

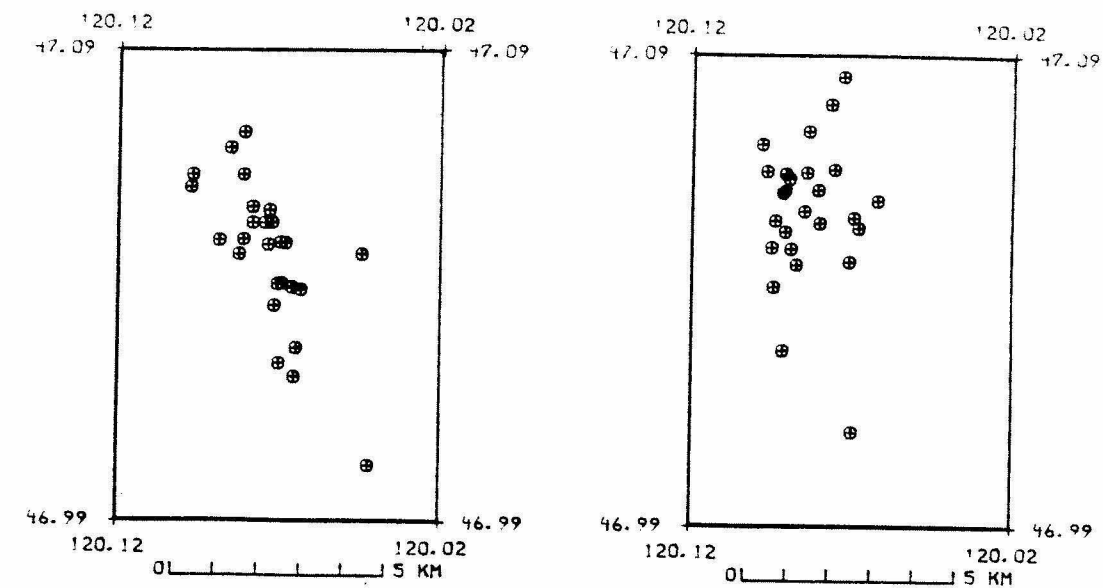


Figure V-1. Comparison of earthquake epicenters using different velocity models. (a) N3 model. (b) modified N3 model.

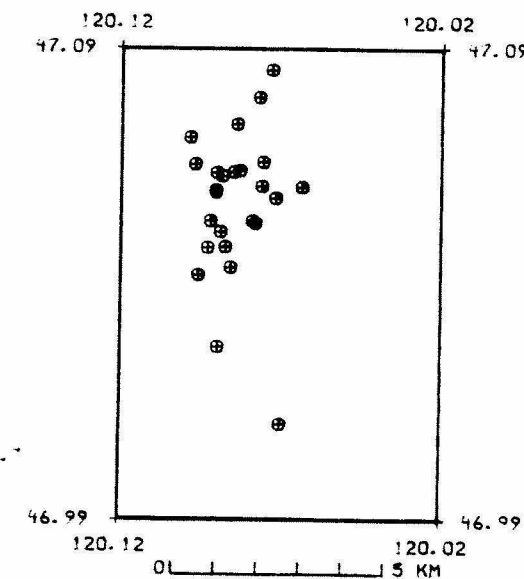


Figure V-2. Epicenters of the Vantage swarm earthquakes using the modified N3 velocity model and holding the depths fixed at 1.0km.

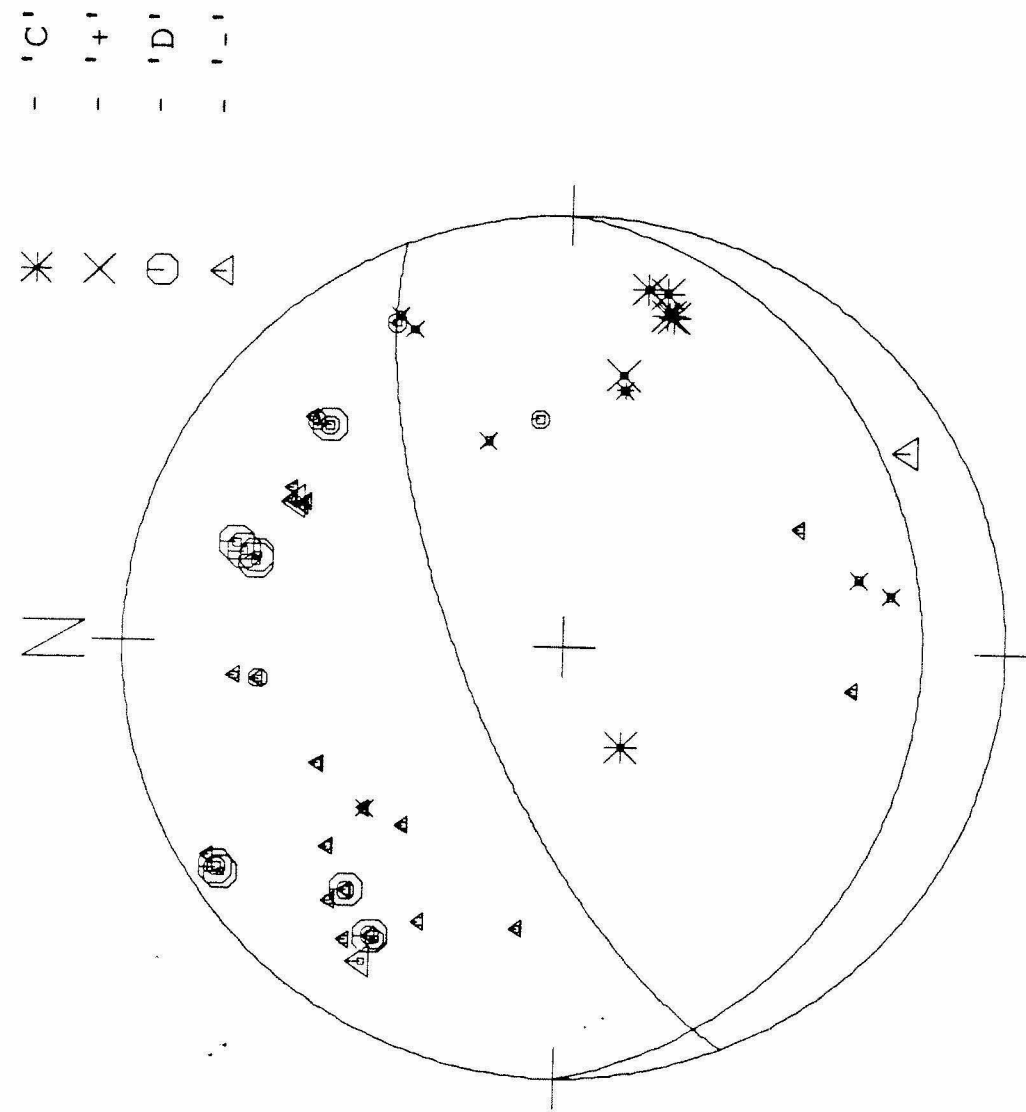


Figure V-3. First motion plot and fault-plane solution of the composite of the seven largest Vantage swarm earthquakes. The plot is an upper hemisphere, equal area stereo projection.

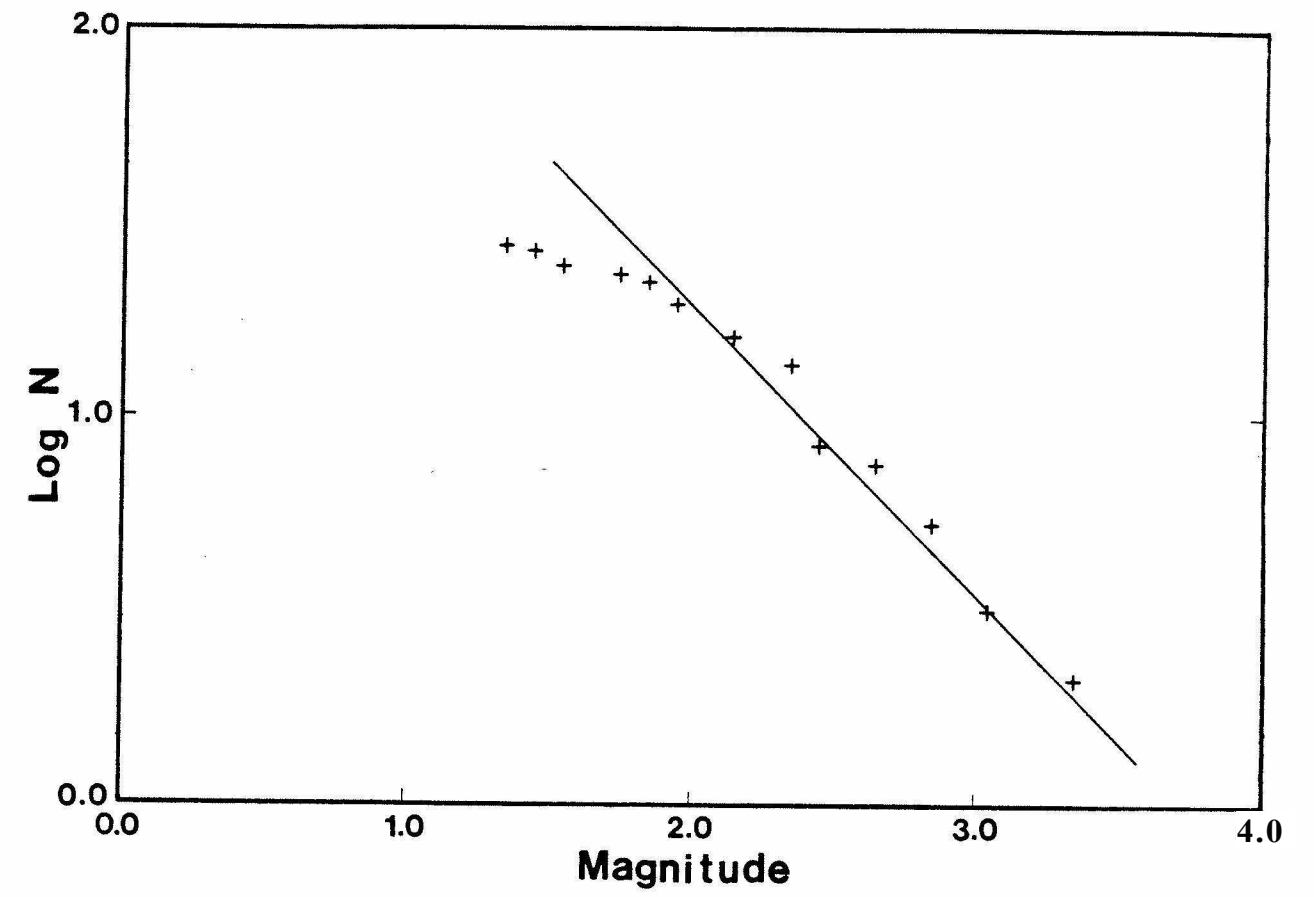


Figure V-4. Log N versus magnitude plot for the Vantage earthquake swarm showing a *b* value of 0.8.

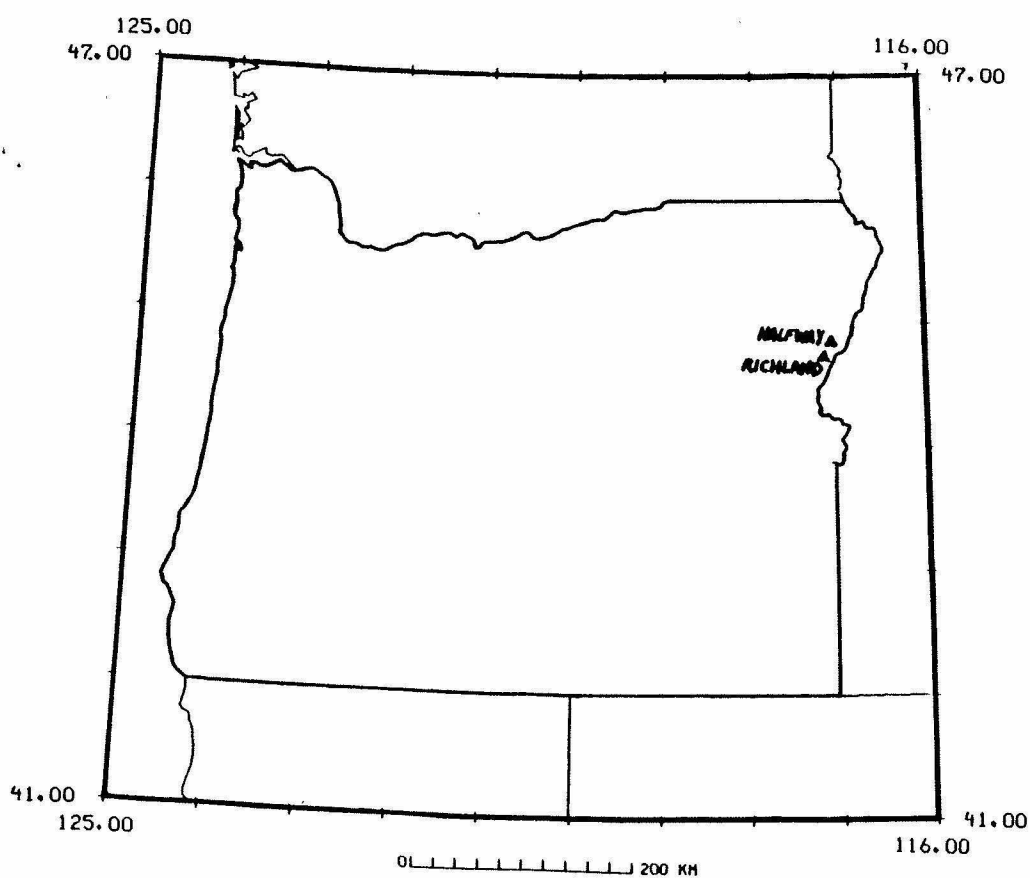


Figure V-5. Index map showing the area of the Powder River earthquake swarm near Richland and Halfway, Oregon.

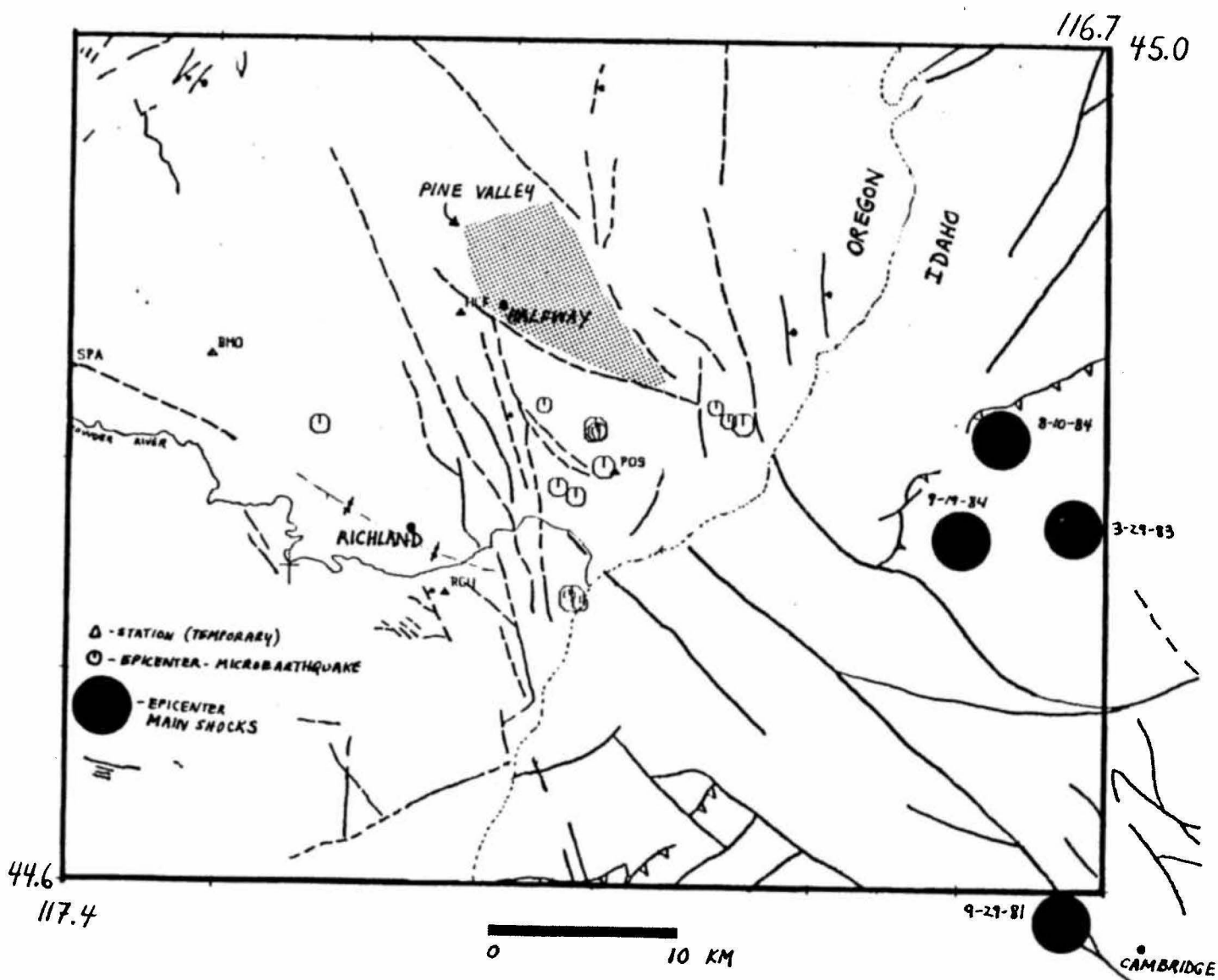


Figure V-6. Detailed map of the area around the Powder River earthquake swarm showing the area of the landslide, mapped surface faults, temporary seismograph stations (triangles), epicenters of the larger events (solid circles) located by permanent stations at some distance, and epicenters of micro-earthquakes (open circles) located by the local temporary stations.

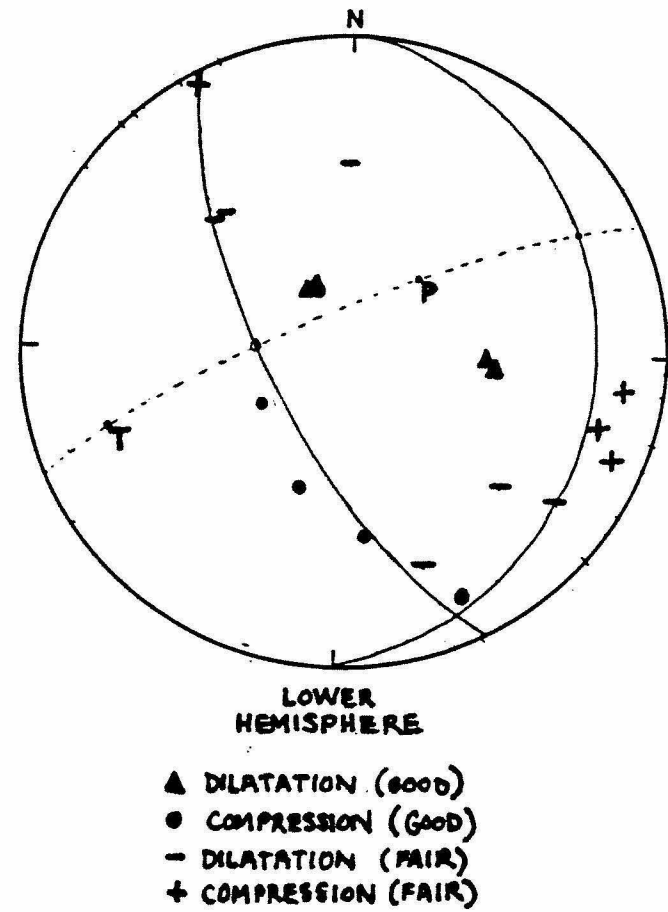


Figure V-7 Composite focal mechanism plot of the best first-motions from the microearthquake records and a few readings from the main shocks of 1983.

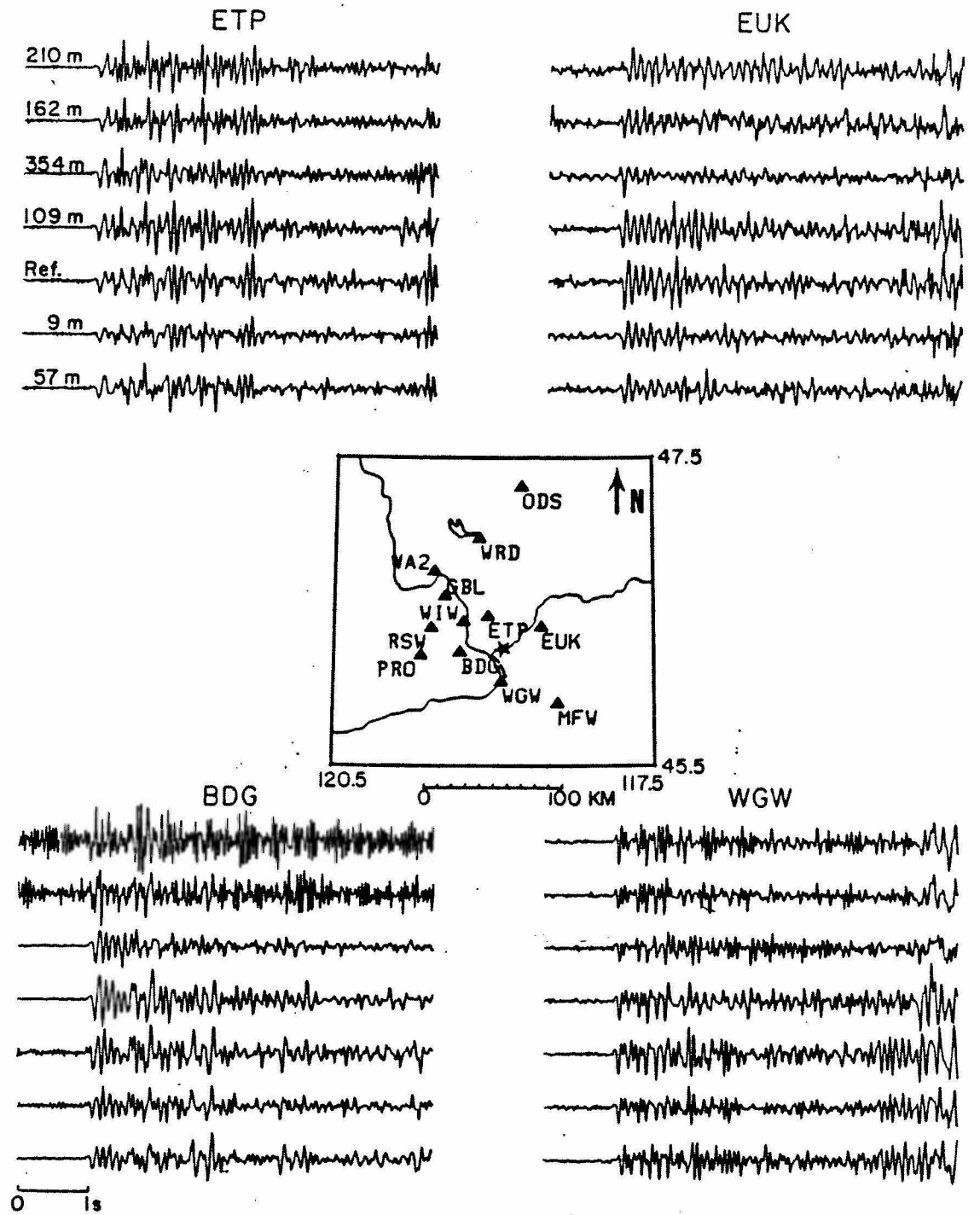


Figure V-8 Map of the area around the Ice Harbor Dam explosion site (star) and the stations used for the relative location procedure. Sample seismograms from 7 different explosions as recorded at four of the stations are shown around the map. The distance of each shot from the reference event is noted on the traces from ETP.

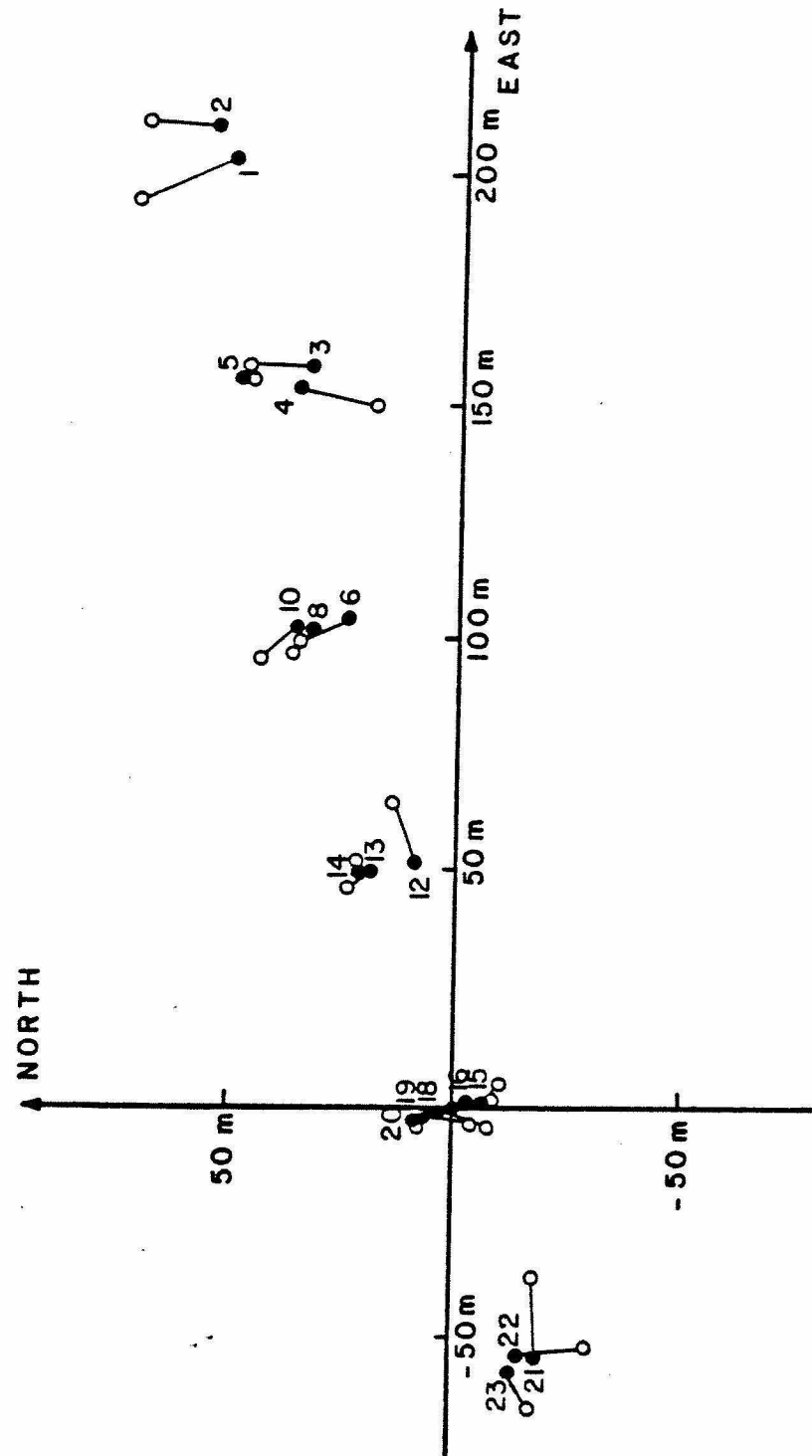


Figure V-9 Detailed map of the explosion site showing the actual locations of each explosion (solid symbols) with the relocated ones (open circle). All events were located relative to event 17, at the origin of the axes.

CATALOG July, 1984 - June, 1985

July 1984											
			LAT	LON	DEPTH	MAG	NS/NP	RMS	Q	MODEL	TYPE
2			47 12.23	119 0.61	9.90*	2.4	7/07	0.25	BC	N3	H
3	1:35	24.4	46 31.73	121 21.97	5.05	1.5	13/14	0.12	AC	C3	
4	3:55	16.47	47 53.47	121 21.47	9.51\$	1.4	4/07	0.12	DD	C3	H
6	5:58	15.50	46 44.19	119 53.12	21.00	1.7	7/07	0.53	DB	E3	
6	12:47	44.92	46 50.66	119 41.56	0.04*	1.8	13/15	0.18	BB	E3	
7	14:0	46.15	47 43.21	120 4.02	4.31	1.9	16/19	0.26	BB	N3	
9	6:14	21.75	46 52.45	121 13.64	0.78\$	1.5	11/13	0.36	CC	C3	
10	0:58	34.02	46 44.65	119 21.59	0.03*	1.7	17/20	0.17	BB	E3	
10	12:41	55.03	46 42.75	119 31.44	0.02*	1.1	5/06	0.16	BD	E3	
10	23:3	13.83	46 25.88	121 48.71	12.83	1.1	10/14	0.06	AC	S3	
12	10:32	40.19	46 52.63	121 13.89	0.98\$	1.9	20/22	0.33	CC	C3	
12	23:17	44.97	46 28.34	123 20.97	0.03*	1.7	6/08	0.32	CD	P3	H
14	0:2	16.91	46 56.91	119 4.76	2.46	1.8	22/22	0.18	BC	E3	
15	8:38	22.36	47 44.17	120 13.02	0.61	2.0	15/19	0.35	CC	N3	
15	23:24	35.62	47 41.95	120 9.07	0.69	1.9	24/28	0.28	BC	N3	
16	0:4	27.52	47 38.51	120 11.75	0.63	2.0	27/32	0.29	BB	N3	
16	7:38	53.90	46 25.73	122 16.30	15.25	2.8	32/37	0.22	BA	S3	
17	17:56	48.60	47 11.27	119 0.40	0.66	2.1	24/24	0.28	BC	N3	
20	3:57	25.82	47 10.33	121 11.66	0.03*	1.7	18/19	0.26	BB	C3	
22	11:46	39.47	47 38.55	120 7.98	0.63	1.7	16/19	0.19	BC	N3	
23	2:41	21.85	46 50.61	119 41.81	0.02*	1.9	18/21	0.16	BB	E3	
23	6:55	51.19	47 42.07	119 53.53	0.51	1.5	8/12	0.40	CB	N3	
23	12:5	40.67	46 44.70	119 22.17	0.02*	1.3	8/09	0.25	BB	E3	
23	12:54	54.29	46 50.19	119 42.04	0.63*	1.4	13/14	0.17	BB	E3	
25	12:25	31.54	45 45.46	122 30.43	16.08	1.8	22/23	0.10	AD	C3	
27	19:18	19.06	47 43.89	120 2.05	4.06	1.5	6/09	0.43	CC	N3	
28	2:25	30.68	46 35.71	120 22.95	0.65	2.7	31/33	0.34	CC	E3	X
28	14:40	53.67	47 31.03	120 36.82	0.88\$	1.9	22/27	0.39	CC	C3	
29	9:22	36.03	47 59.23	121 29.72	2.51\$	2.2	13/16	0.18	BC	C3	
29	13:15	40.61	46 25.94	122 16.83	14.68	0.7	16/22	0.11	AA	S3	
29	22:39	62.17	45 44.91	122 31.21	15.73	1.7	16/17	0.08	BD	C3	
Aug 1984											
DAY	TIME	SEC	LAT	LON	DEPTH	MAG	NS/NP	RMS	Q	MODEL	TYPE
1	14:11	53.38	45 58.75	122 35.28	10.90	1.5	14/16	0.17	BD	C3	
3	19:13	57.30	45 54.45	119 10.42	0.03*	2.4	16/16	0.25	BC	E3	
5	13:2	23.08	46 5.17	119 58.89	8.51#	1.6	4/04	1.99	DD	E3	
5	19:11	50.73	46 26.82	122 15.66	11.26	3.1	35/37	0.26	BA	S3	
7	1:12	38.03	45 56.13	123 31.63	10.83*	2.1	21/23	0.19	BD	P3	
9	6:23	14.00	46 25.57	122 17.40	15.02	1.1	21/31	0.14	AA	S3	
10	21:11	48.98	46 7.51	119 47.27	0.02*	2.5	18/18	0.16	BC	E3	P
11	1:6	23.62	46 10.40	122 18.70	14.01	0.8	13/21	0.07	AA	S3	
14	9:15	14.51	48 46.30	119 29.92	10.75	1.4	9/10	0.17	CD	N3	
14	21:44	11.23	47 7.15	118 46.04	5.51	2.6	22/22	0.25	BD	N3	P
16	1:56	45.92	47 34.67	120 17.84	6.74	1.8	4/07	0.04	AD	N3	
16	4:20	23.16	47 51.20	119 16.57	5.84	1.9	8/11	0.41	CC	N3	